We are IntechOpen,
the world's leading publisher of
Open Access books
Built by scientists, for scientists

4,800
Open access books available

122,000
International authors and editors

135M
Downloads

Our authors are among the

154
Countries delivered to

TOP 1%
most cited scientists

12.2%
Contributors from top 500 universities

BOOK
CITATION
INDEX
CLARIVATE ANALYTICS
INDEXED

WEB OF SCIENCE™

Selection of our books indexed in the Book Citation Index
in Web of Science™ Core Collection (BKCI)

Interested in publishing with us?
Contact book.department@intechopen.com

Numbers displayed above are based on latest data collected.
For more information visit www.intechopen.com

Mass Transfer in Bioreactors

Ma. del Carmen Chávez[1], Linda V. González[2], Mayra Ruiz[3], Ma. de la Luz
X. Negrete[4], Oscar Martín Hernández[5] and Eleazar M. Escamilla[6]

*[1]Facultad de Ingeniería Química, Universidad Michoacana de San Nicolás de Hidalgo,
Francisco J Mújica s/n, Col. Felicitas del Río, 58060, Morelia, Michoacán.
[2]Centro de Investigación y Desarrollo Tecnológico en Electroquímica, Parque
Tecnológico Querétaro Sanfandila, 76703 Sanfandila, Pedro Escobedo, Qro.,
[3]Facultad de Ingeniería Química, Benemérita Universidad Autónoma de Puebla.
4 sur 104 centro histórico C.P. 72000, Puebla.,
[4]Departamento de Ingeniería Ambiental, Instituto Tecnológico de Celaya, Ave.
Tecnológico y Antonio García Cubas S/N, Celaya, Gto., C.P. 38010,
[5]Universidad Autónoma de Sinaloa. Facultad de Ciencias Químico Biológicas.
Ciudad Universitaria, C.p. 80090, Culiacán, Sinaloa.
[6]Instituto Tecnológico de Celaya, Departamento de Ingeniería Química, Ave.
Tecnológico y Antonio García Cubas S/N, Celaya, Gto., C.P. 38010,Sinaloa.
México*

1. Introduction

The study of transport in biological systems is complicated for two reasons: 1. because each system is different, we cannot generalize it and 2. Because always take place in more than one phase. If we talk about microorganism, there is a range of them with physicochemical and biological characteristics very different, and certain microorganisms can be filamentous and can grow branched or dispersed, in some the viscosity and density increases with time. In some times their maximum growth rate is achieved in two hours while others in 15 days. Some are affected by the light, others agitation rate, others require air for developing others not. If we talk about production of plants by tissue culture systems have become more complex, that the transport properties are affected by agitation rate, type of agitation, the growth of tissues. To design the bioreactors of these biological systems requires knowledge of the nature of what is to be produced, the dynamics of transport, rheology, to decide what type of reactor we can used. Biological fluids such reactors behave as highly non-Newtonian systems and as such require special treatment. This paper will discuss three types of reactors: air-lift, packed column and fluidized bed and stirred tank, where case studies are applied to biological systems. 1. Production of Gibberellic acid and Bikaverin 2. Biodegradation of azodyes in textile industry and 3. Gibberellins Production. It is intended that in these three cases brought to appreciate as engineering parameters are evaluated where they involve the transport mass balances and the type of bioreactor and feature you in l fluid. On the other hand show a combination of experimental results and simulations with mathematical models developed to strengthen the knowledge of chemical engineering applied to biological systems.

2. Case I. Hydrodynamics, mass transfer and rheological studies of gibberellic acid production in an airlift bioreactor

2.1 Introduction

Gibberellic acid is an endogenous hormone in higher plants, belonging to the group of gibberellins, and also a product of the secondary metabolism in certain fungi. Approximately 126 gibberellins have been characterized (Tudzynski 1999; Shukla et al. 2003) but only a few are commercially available. Gibberellic acid is the most important and its effects on higher plants are: marked stem elongation, reversal of dwarfism, promotion of fruit setting, breaking of dormancy, acceleration of seed fermentation, among others (Brückner and Blechschmidt 1991; Tudzynski 1999). Currently, gibberellic acid is microbiologically produced in a submerged culture (SmF) fashion but another fermentation techniques such as solid sate fermentation or with immobilized mycelium are also reported (Heinrich and Rehm 1981; Jones and Pharis 1987; Kumar and Lonsane 1987, 1988; Nava Saucedo et al. 1989; Escamilla et al. 2000; Gelmi et al. 2000, 2002). Nevertheless stirred tank bioreactors with or without a fed-batch scheme have been the most employed in gibberellic acid production. Other geometries and type of bioreactors have also been reported. Only Chavez (2005) has described gibberellic acid production employing an airlift bioreactor. Airlift bioreactors are pneumatically agitated and circulation takes place in a defined cyclic pattern through a loop, which divides the reactor into two zones: a flow-upward and a flow-downward zone. The gas-sparged zone or the riser has higher gas holdup than the relatively gas-free zone, the downcomer, where the flow is downward (Gouveia et al. 2003). Practical application of airlift bioreactors depends on the ability to achieve the required rates of momentum; heat and mass transfer at acceptable capital and operating costs. The technical and economic feasibility of using airlift devices has been conclusively established for a number of processes and these bioreactors find increasing use in aerobic fermentations, in treatment of wastewater and other similar operations. The simplicity of their design and construction, better defined flow patterns, low power input, low shear fields, good mixing and extended aseptic operation, made possible by the absence of stirrer shafts, seals and bearings, are important advantages of airlift bioreactors in fermentation applications (Chisti 1989).

Even though gibberellic acid has been produced on an industrial scale since the last century, hydrodynamics, mass transfer and rheological studies are sparse. Flow regime, bubble size distribution, and coalescence characteristics, gas holdup, interfacial mass transfer coefficients, gas–liquid interfacial area, dispersion coefficients and heat transfer coefficients are important design parameters for airlift bioreactors. A thorough knowledge of these interdependent parameters is also necessary for a proper scale-up of these bioreactors (Shah et al. 1982). Besides hydrodynamics and mass transfer studies, rheological studies are important since in many chemical process industries, the design and performance of operations involving fluid handling like mixing, heat transfer, chemical reactions and fermentations are dependent on the rheological properties of the processed media (Brito-De la Fuente et al. 1998). Mycelial fermentation broths present challenging problems in the design and operation of bioreactors since the system tends to have highly non-Newtonian flow behaviour and this has a very significant effect on mixing and mass transfer within the bioreactor.

The main objective of this work was to study hydrodynamic, mass transfer and rheological aspects of gibberellic acid production by *Gibberella fujikuroi* in an airlift reactor.

2.2 Materials and methods

Microorganism and inoculum preparation *Gibberella fujikuroi* (Sawada) strain CDBB H-984 maintained on potato dextrose agar slants at 4_C and sub-cultured every 2 months was used

in the present work (Culture collection of the Department of Biotechnology and Bioengineering, CINVESTAV-IPN, Mexico). Fully developed mycelia materials from a slant were removed by adding an isotonic solution (0.9% NaCl). The removed mycelium was used to inoculate 300 ml of fresh culture medium contained in an Erlenmeyer flask. The flask was placed in a radial shaker (200 rev min–1) for 38 h at 29 ± 1_C. Subsequent to this time; the contents of the flask were used to inoculate the culture medium contained in the airlift bioreactor. The culture medium employed for the inoculum preparation is reported by Barrow et al. (1960).

Batch culture in the airlift bioreactor

An airlift bioreactor (Applikon, Netherlands, working volume, 3.5 l) was employed in the present work. It consists of two concentric tubes of 4.0 and 5.0 cm of internal diameter with a settler. The air enters the bioreactor through the inner tube. A jacket filled with water allowing temperature control surrounds the bioreactor. It is also equipped with sensors of pH and dissolved oxygen to control these variables. Moreover it allows feed or retiring material from the bioreactor employing peristaltic pumps. Typical culture medium contained glucose (50 g l^{-1}), NH_4Cl (0.75 g l^{-1}) or NH_4NO_3 (1.08 g l^{-1}), KH_2PO_4 (5 g l^{-1}), $MgSO_4$. 7 H_2O (1 g l^{-1}) and trace elements (2 ml l^{-1}). A stock solution of the trace elements used contained (g l^{-1}) 1.0 Fe SO_4. 7 H_2O, 0.15 $CuSO_4$. 5 H_2O, 1.0 $ZnSO_4$. 7 H_2O, 0.1 $MnSO_4$. 7 H_2O, 0.1 $NaMoO_4$, 3.0 EDTA (Na_2 salt) 1 l of distilled water, and hydrochloric acid sufficient to clarify the solution (Barrow et al. 1960). During the fermentation period, the pH was controlled to 3.0, temperature to 29°C and aeration rate to 1.6 vvm. These conditions promoted gibberellic acid production with the studied strain but they are not optimized values. About 30 ml subsamples were withdrawn from the bioreactor at different times and were used to perform rheological studies. Biomass concentration was quantified by the dry weight method.

2.3 Hydrodynamics and mass transfer studies

Gas holdup was determined in the actual culture medium using an inverted U-tube manometer as described by Chisti (1989). Liquid velocities in the riser were determined measuring the time required for the liquid to travel through the riser by means of a pulse of concentrated sulphuric acid using phenolphthalein as an indicator; the same was done for the downcomer. The mixing time was calculated as the time required obtaining a pH variation within 5% of the final pH value. For doing this, pH variation was followed after injection of a pulse of a concentrated solution of ammonium hydroxide. The volumetric mass transfer coefficient was determined employing the gassing-out method as described elsewhere (Quintero 1981).

2.4 Rheological studies

Rheological studies of fermentation broth were performed in a rotational rheometer (Haake, Model CV20N) equipped with a helical impeller to perform torque measurements. This type of geometry is appropriate when dealing with complex fluids and the measurement methodology is reported by Brito-de la Fuente et al. (1998). Rheological results, like hydrodynamics and mass transfer, are given as the average of two replicates for each sample. All the experiments were carried out in triplicate and the results that are presented are an average.

2.5 Results and discussion

Gas holdup

The importance of gas holdup is multifold. The gas holdup determines the residence time of the gas in the liquid and, in combination with the bubble size, influences the gas–liquid interfacial area available for mass transfer. The gas holdup impacts upon the bioreactor design because the total design volume of the bioreactor for any range of operating conditions depends on the maximum gas holdup that must be accommodated (Chisti 1989). Figure 1 shows the gas holdup (ε) variation with superficial gas velocity in the riser (v_{gr}). Experimental data were fitted to a correlation of the type of Eq. 1.

$$F = A \, v_{gr}^{B} \tag{1}$$

Where F could be the gas holdup (ε), the liquid velocity in the riser (v_{lr}), liquid velocity in the downcomer (v_{ld}) or the volumetric mass transfer coefficient (k_La). This type of correlation has been applied by many investigators (Shah et al. 1982; Godbole et al. 1984; Chisti 1989; Gravilescu and Tudose 1998; Abashar et al. 1998) and was derived empirically. Chisti (1989) presented an analysis for Newtonian and non-Newtonian fluids where shows the theoretical basis of Eq. 1 (for the gas holdup case). He found that parameters A and B were dependent on the flow regime and on the flow behaviour index of the fluid. Moreover, parameter A is dependent on the consistency index of the fluid, on the fluid densities and on the gravitational field. Equation 2 was obtained from fitting experimental data.

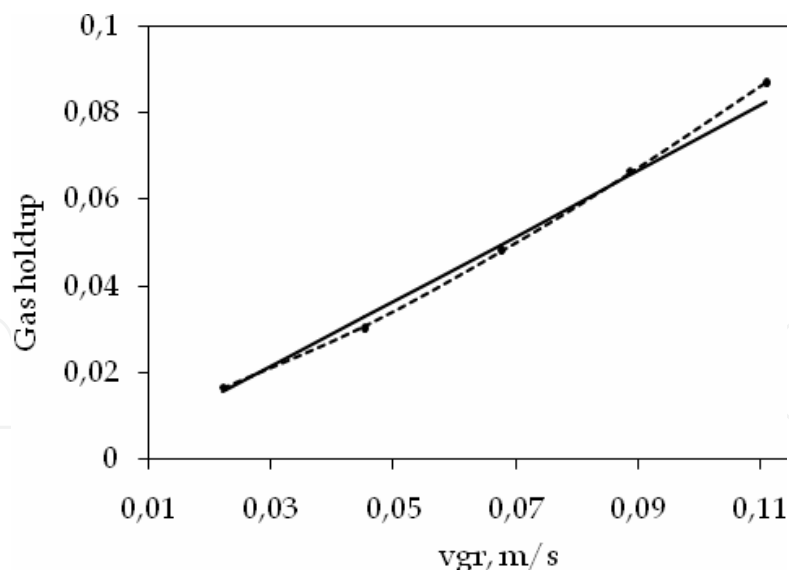$$\varepsilon = 0.7980 \, v_{gr}^{1.0303} \tag{2}$$

Fig. 1. Gas holdup variation with superficial gas velocity in the riser.
• Experimental data ––– Equation 2 --- Equation 12

An increase in superficial gas velocity in the riser implies an increase in the quantity of gas present in the riser, that is, an increase of gas fraction in the riser (Chisti 1989; Gravilescu and Tudose 1998). Chisti (1989) reports a correlation that calculates the value of B in Eq. 1 (for the gas holdup case). The value obtained employing this correlation is 1.2537.

Gravilescu and Tudose (1998) present a similar correlation, which predicts a value of 0.8434 for B. The B value obtained in the present work is between the B values obtained from these correlations that employ the flow behaviour index obtained from rheological studies. Shah et al. (1982) reported that B values in Eq. 1 oscillate between 0.7 and 1.2.

Liquid velocity

The liquid circulation in airlift bioreactors originates from the difference in bulk densities of the fluids in the riser and the downcomer. The liquid velocity, while itself controlled by the gas holdups in the riser and the downcomer, in turn affects these gas holdups by either enhancing or reducing the velocity of bubble rise. In addition, liquid velocity affects turbulence, the fluidreactor wall heat transfer coefficients, the gas–liquid mass transfer and the shear forces to which the microorganism are exposed. Figure 2 shows liquid velocities variation in the riser and the downcomer as a function of superficial gas velocity in the riser. Liquid velocities in the riser (v_{lr}) and in the downcomer (v_{ld}) were fitted to correlations of the type of Eq. 1 and Eqs. 3 and 4 were obtained.

$$v_{lr} = 1.3335 \, v_{gr}^{0.3503} \tag{3}$$
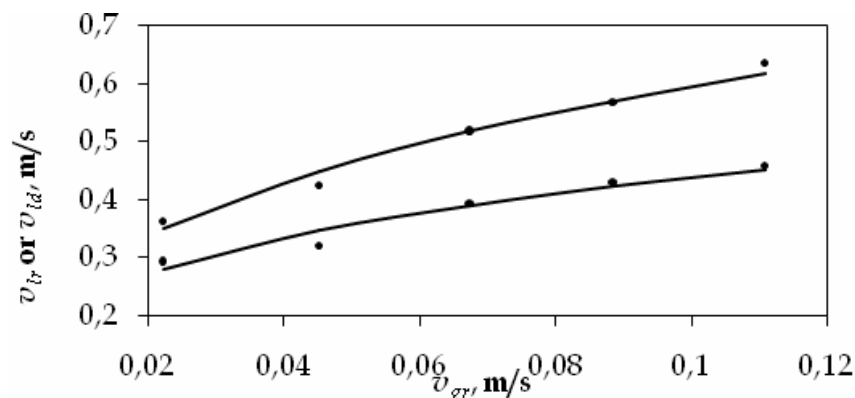
$$v_{ld} = 0.8716 \, v_{gr}^{0.2970} \tag{4}$$

Fig. 2. Liquid velocities as a function of superficial gas velocity in the riser.
• Experimental data –– Equation 3 or 4

The B value in Eq. 1 must be close to 0.3333 as was reported by Freitas and Teixeira (1998) for the liquid velocity in the riser, Kawase (1989) theoretically derived this value. The B value obtained in the present work is closer to 0.3333. Freitas and Teixeira (1998) also showed that the B values for the liquid velocity in the downcomer were lower than the B value for the liquid velocity in the riser, which agrees with the results obtained in this work. Liquid velocities in the riser and in the downcomer increase with an increase in gas velocity in the riser due to an increase in the density difference of the fluids in the riser and the downcomer.

Mixing time

Mixing in airlift bioreactors may be considered to have two contributing components: back mixing due to recirculation and axial dispersion in the riser and
downcomer due to turbulence and differential velocities of the gas and liquid phases (Choi et al. 1996).

Mixing time is used as a basis for comparing various reactors as well as a parameter for scaling up (Gravilescu and Tudose 1999). Figure 3 shows the mixing time variation with the superficial gas velocity in the riser. Once again, the mixing time variation was fitted to a correlation of the type of Eq. 1 and Eq. 5 was obtained.

$$t_m = 5.0684 \, v_{gr}^{-0.3628} \qquad\qquad (5)$$

Choi et al. (1996) reported a B value in Eq. 5 of –0.36 while Freitas and Teixeira (1998) reported a B value equal to –0.417. The B value obtained in this work is similar to the value reported by Choi et al. (1996). The mixing time decreases with an increase in superficial gas velocity in the riser since the fluid moves more often to the degassing zone where most of the mixing phenomenon takes place, due to the ring vortices formed above the draught tube (Freitas and Teixeira 1998).

Volumetric mass transfer coefficient

One of the major reasons that oxygen transfer can play an important role in many biological processes is certainly the limited oxygen capacity of the fermentation broth due to the low solubility of oxygen. The volumetric mass transfer coefficient (k_La) is the parameter that characterizes gas-liquid oxygen transfer in bioreactors. One of the commonest employed scale-up criteria is constant k_La. The influences of various design (i.e., bioreactor type and geometry), system (i.e., fluid properties) and operation (i.e., liquid and gas velocities) variables on k_La must be evaluated so that design and operation are carried out to optimize k_La (Chisti, 1989).
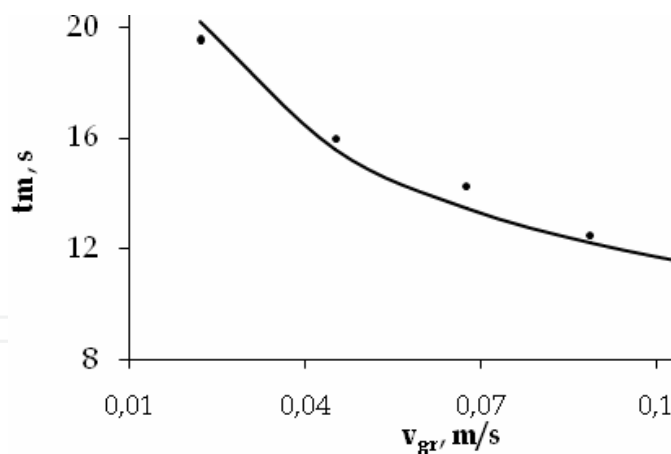

Fig. 3. Mixing time as a function of superficial gas velocity in the riser.

The value of the volumetric mass transfer coefficient determined for a microbial system can differ substantially from those obtained for the oxygen absorption in water or in simple aqueous solutions, i.e., in static systems with an invariable composition of the liquid media along the time. Hence k_La should be determined in bioreactors which involve the actual media and microbial population (Tobajas and García-Calvo, 2000). Figure 4 shows the volumetric mass transfer coefficient variation with the superficial gas velocity in the riser. Experimental data shown in Figure 4 were fitted to a correlation of the type of Equation 1 and Equation 6 was obtained.

$$k_L a = 0.4337 \ v_{gr}^{1.2398} \tag{6}$$

Barboza *et al.*, (2000) report a *B* value in Equation 6 equal to 1.33 and Schügerl *et al.*, (1977) report a value of 1.58. The value of 1.2398, obtained in this work, is close to these last values.
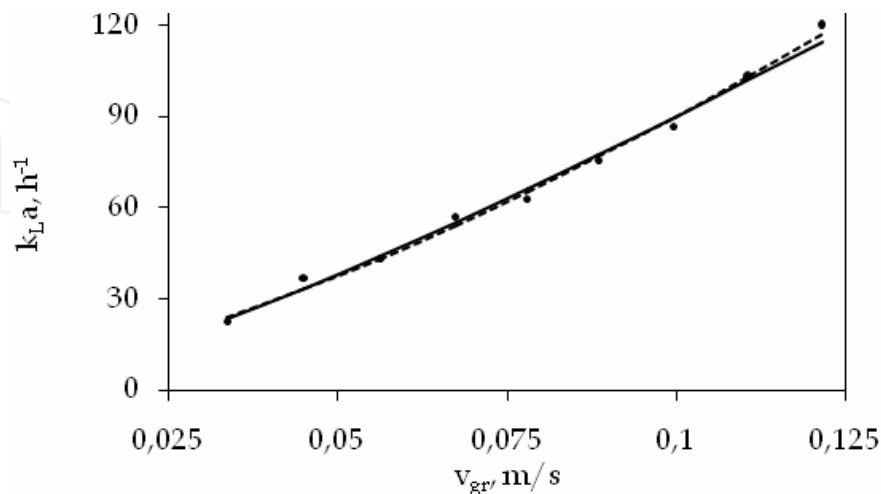

Fig. 4. Effect of the superficial gas velocity in the riser on $k_L a$.

Volumetric mass transfer coefficient ($k_L a$) increases with an increase in superficial gas velocity in the riser due to an increase in gas holdup which increases the available area for oxygen transfer. Moreover an increase in the superficial gas velocity in the riser increases the liquid velocity which decreases the thickness of the gas-liquid boundary layer decreasing the mass transfer resistance. Figure 5 shows the evolution of $k_L a$ through fermentation course employing two different nitrogen sources. The $k_L a$ decreases in the first hours of fermentation and reaches a minimum value at about 24 hours. After this time the $k_L a$ starts to increase and after 48 hours of fermentation it reaches a more or less constant value which remains till the end of fermentation process. This behaviour is similar irrespective of the nitrogen source and will be discussed with the rheological results evidence.
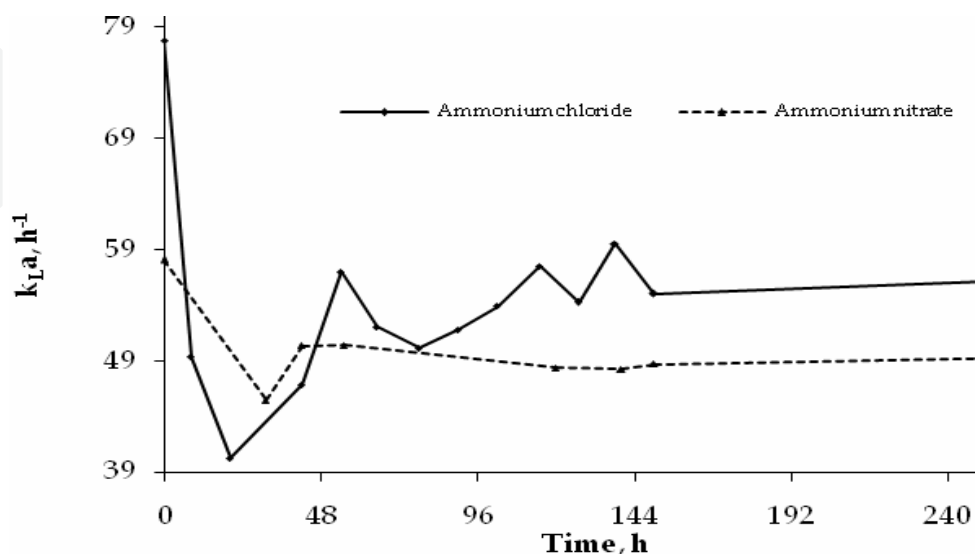

Fig. 5. $k_L a$ through fermentation time in the airlift bioreactor.

Figure 6 shows the relation between gas holdup and k_La. McManamey and Wase (1986) point out that the volumetric mass transfer coefficient is dependent on gas holdup in pneumatically agitated systems. The later was experimentally determined in bubble columns by Akita and Yoshida (1973) and Prokop *et al.*, (1983). Shah *et al.*, (1982) mention that this was expectable since both the volumetric mass transfer coefficient and the gas holdup present similar correlations with the superficial gas velocity. McManamey and Wase (1996) proposed a correlation similar to Equation 1 to relate volumetric mass transfer coefficient with gas holdup. Equation 7 presents the obtained result.

$$k_La = 0.2883\ \varepsilon^{0.9562} \tag{7}$$

Akita and Yoshida (1973) and Prokop *et al.* (1983) found that the exponent in Equation 7 oscillates between 0.8 and 1.1.

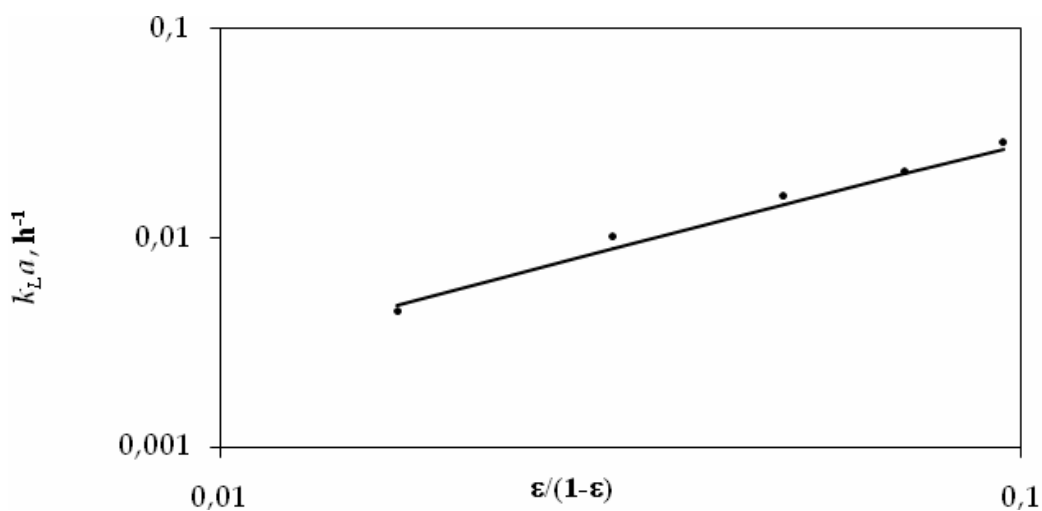$$\ln k_La = \ln\left(6\frac{k_L}{d_B}\right) + \ln\frac{\varepsilon}{(1-\varepsilon)} \tag{8}$$

Fig. 6. k_La vs. gas holdup in the airlift bioreactor, unit slope.

It is well known (Chisti, 1989) that logarithmic scale plots of k_La vs. $\varepsilon/(1-\varepsilon)$ for any particular data set should have a unit slope according to Equation 8. Where k_L is the mass transfer coefficient and d_B is the bubble diameter. Even though the later is a generally known fact, few investigators determined these slopes for their data to ascertain the validity of their experimental results. Figure 6 shows this analysis for the experimental data of the present work obtaining a slope of 1.034. Chisti (1989) shows the same analysis for two different data set and obtained slopes of 1.020 and 1.056.

A rearrangement of Equation 8 leads to Equation 9 which results are shown in Figure 7. As is showed in the Figure 7 the gas superficial velocity practically did not affect the k_L/d_B values, therefore it can be taken as a value average and constant to slant the superficial velocity changes.

$$\frac{k_L}{d_B} = \frac{k_La(1-\varepsilon)}{6\varepsilon} \tag{9}$$

The average value of k_L/d_B obtained in the present work is 0.050 s^{-1}. Chisti (1989) performed a similar analysis for 97 data points obtained from several different reactors and found an average value of 0.053 s^{-1}. The foregoing observations have important scale-up implications. In large industrial fermenters the k_La determination is not only difficult, but there is uncertainty as to whether the measured results reflect the real k_La or not. The gas holdup measurements on these reactors are relatively easy to carry out, however. Thus, Equation 9 can help to estimate k_La in these reactors once gas holdup measurements have been made (Chisti, 1989).
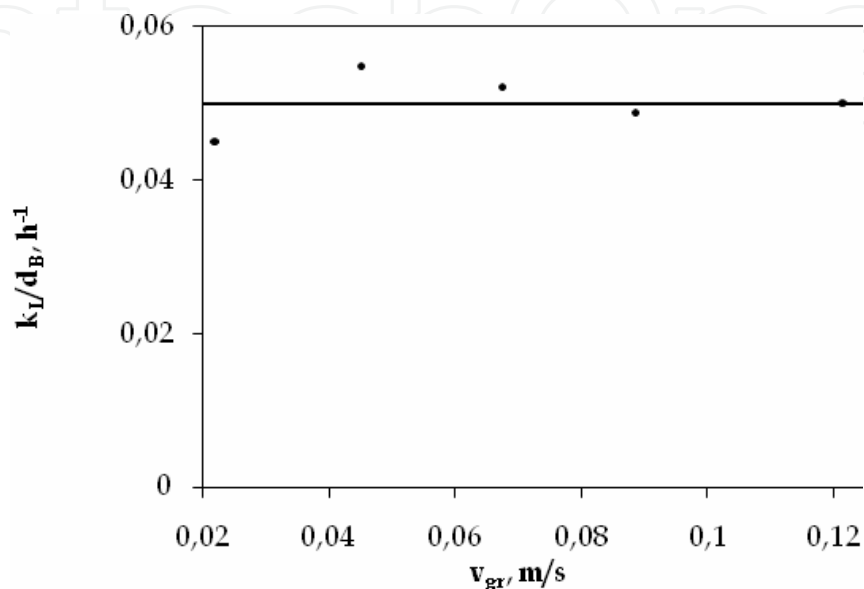

Fig. 7. The k_L/d_B ratio as a function of superficial gas velocity.

2.6 Rheology

Rheological parameters such as the flow index (n) and the consistency index (K) depend on such factors as the concentration of solids in the broth, the morphology (length, diameter, degree of branching, shape) of the particles, the growth conditions (flexibility of cell wall and particle), the microbial species and the osmotic pressure of the suspending liquid, among others possible factors. For the case of mycelial cultures, as the biomass concentration increases the broth becomes more viscous and non-Newtonian; leading to substantial decreases in oxygen transfer rates. This effect is often important since for many aerobic processes involving viscous non-Newtonian broths oxygen supply is the limiting factor determining bioreactor productivity (Moo-Young et al., 1987). Apparent viscosity is a widely used design parameter which correlates mass transfer and hydrodynamic parameters for viscous non-Newtonian systems (Al-Masry and Dukkan, 1998).

It is worth to mention that the present work uses impeller viscometry for performing rheological studies avoiding the use of other geometries, i.e., concentric tubes or cone and plate, overcoming associated problems with these geometries such sedimentation, solids compacting and jamming between measuring surfaces or pellet destruction (Metz et al., 1979). Impeller viscometry was used to obtain torque data at different velocities of the impeller, these data were transformed to shear stress (τ) and shear rate (γ) data and typical results are shown in Figure 8. As can be seen in Figure 8, the experimental data follow a straight line and can be represented by the Ostwald-de Waele model (Equation 10).
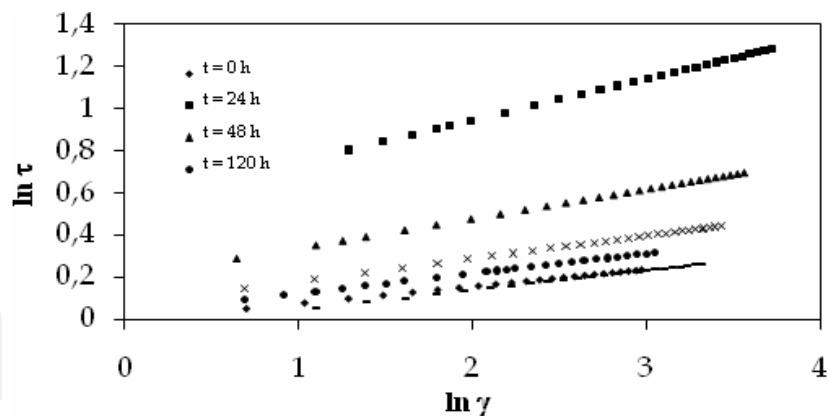
$$\tau = K\gamma^{n} \tag{10}$$

Fig. 8. Typical rheogram employing impeller viscometry

Rheograms obtained from fermentations employing different nitrogen source show a pseudo plastic behaviour for the culture medium during the fermentation period since the exponent, n, in Equation 10 is always lower than unity. Figure 9 shows the results of consistency and flow indexes for the different fermentations, employing ammonium chloride or ammonium nitrate as nitrogen source, where similar results were obtained.
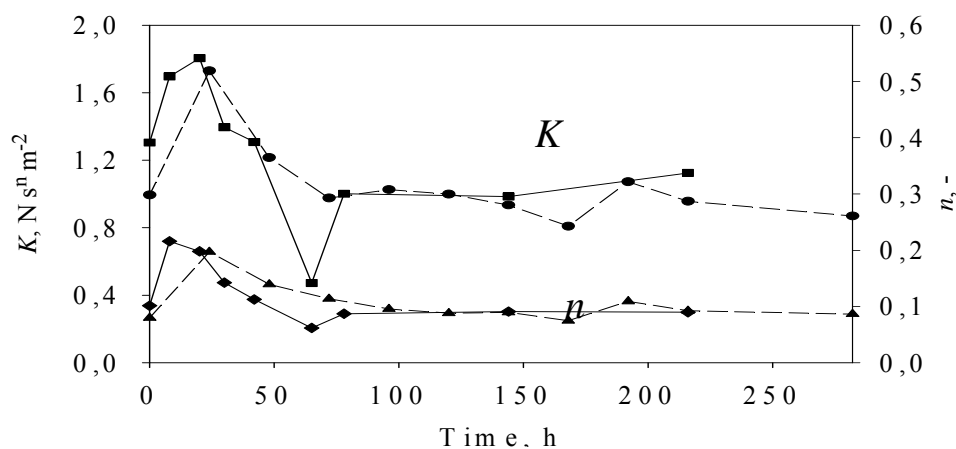

Fig. 9. K and n through fermentation time in the airlift bioreactor • K for ammonium nitrate ▲ n for ammonium nitrate ■ K for ammonium chloride ◆ n for ammonium chloride.
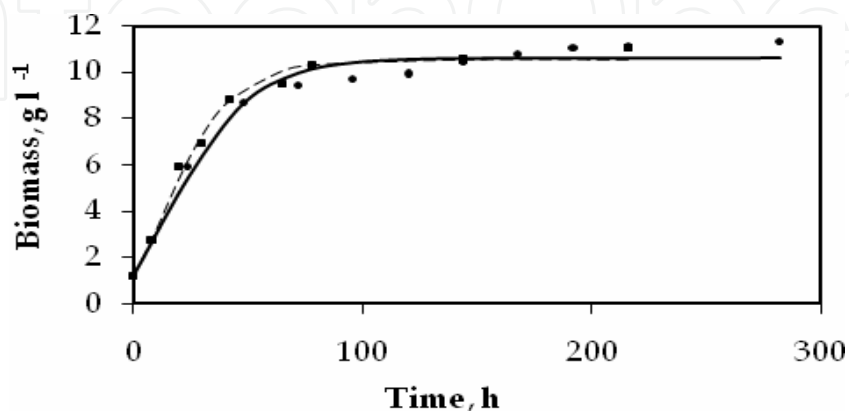

Fig. 10. Growth kinetics employing ammonium chloride (■) or ammonium nitrate (•) as nitrogen source.

Figure 10 shows the growth kinetics of *Gibberella fujikuroi* obtained during different fermentations. As can be seen in Figure 10, the growth kinetics is similar irrespective of the employed nitrogen source. Experimental data where fitted to two-parameter Gompertz model proposed by Chavez-Parga et al., (2005). As can be seen in Figure 10, there is no lag phase and exponential growth of mycelia starts immediately and ceases during the first 24 hours of fermentation. The later causes the medium viscosity to increase (K and n increase in Figure 9) which causes a k_La decrease in Figure 5. After 24 hours of fermentation, the formation of pellets by the fungus starts to occur reflected in a decrease of medium viscosity (K and n start to decrease in Figure 9) and hence an increase in k_La value in Figure 5. After 72 hours of fermentation the medium viscosity was practically unchanged (K and n remain constant in Figure 9) because the stationary growth phase is reached by the fungus reflected in practically constant values of medium viscosity and k_La. Also, after 72 hours of fermentation, the pellet formation process by the fungus stops.

Figure 11 shows the correlation between consistency and flow indexes with biomass concentration. Experimental data were fitted to Equations 11 and 12 proposed in the present work. Optimized values for constants in Equations 11 and 12 are summarized in Table 1.

$$K = \frac{c_1}{\left(1 + \dfrac{c_2}{x}\right) + \left(\dfrac{x}{c_3}\right)^2} \tag{11}$$

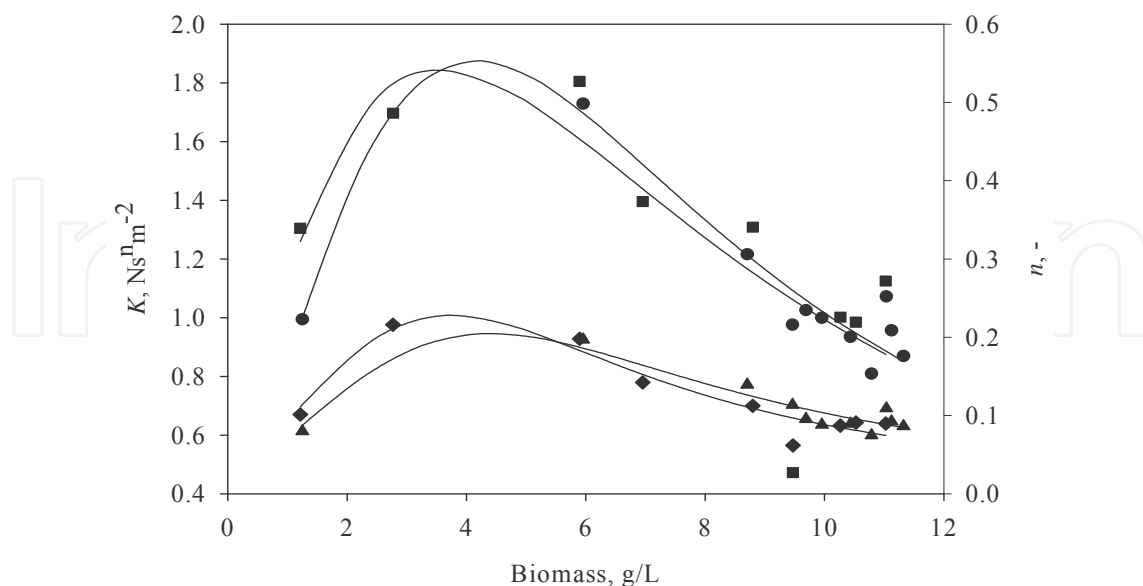$$n = \frac{c_1}{\left(1 + \dfrac{c_2}{x}\right) + \left(\dfrac{x}{c_3}\right)^2} \tag{12}$$

Fig. 11. K and n as a function of biomass concentration in the airlift bioreactor.
• K for ammonium nitrate ▲ n for ammonium nitrate ■ K for ammonium chloride
◆ n for ammonium chloride.

Consistency index			
Nitrogen source	c_1	c_2	c_3
Ammonium nitrate	6.31	6.55	4.69
Ammonium chloride	3.43	2.05	6.67
Flow index			
Nitrogen source	c_1	c_2	c_3
Ammonium nitrate	7.64	106.49	1.27
Ammonium chloride	7.63	80.91	1.14

Table 1. Optimized values found for constants of Equations 11 and 12.

With the aid of rheological studies is possible to use correlations of the type of Equation 13 to relate gas holdup and volumetric mass transfer coefficient with fermentation medium viscosity (Godbole *et al.*, 1984; Halard *et al.*, 1989; Al-Masry and Dukkan, 1998; Barboza *et al.*, 2000) to obtain Equations 14 and 15.

$$F = A v_{gr}^{B} \mu_{app}^{C} \tag{13}$$

$$k_L a = 0.0036 \, v_{gr}^{0.3775} \mu_{app}^{-0.5488} \tag{14}$$

$$\varepsilon = 0.0072 \, v_{gr}^{0.2381} \mu_{app}^{-0.5703} \tag{15}$$

Figures 1 and 4 show experimental data fitting for gas holdup and $k_L a$, respectively. As it was expectable, Equations 14 and 15 present a better fit to experimental data than that obtained with the aid of Equations 2 and 3 due to the existence of an extra adjustable parameter.

2.7 Conclusions

In the present work preliminary hydrodynamics, mass transfer and rheological studies of gibberellic acid production in an airlift bioreactor were achieved and basic correlations between gas holdup, liquid velocity in the riser, and liquid velocity in the downcomer, mixing time and volumetric mass transfer coefficient with superficial gas velocity in the riser were obtained. Adjustable parameters calculated for each variable were compared with literature reported values and a good agreement was obtained. Gassing out method was successfully applied in determining volumetric mass transfer through fermentation time employing two different nitrogen sources. Irrespective of the nitrogen source the volumetric mass transfer behaviour was similar and it was explained in terms of the fungus growth and changes in its morphology which affect the culture medium rheology. Pellet formation by the fungus was used to explain the increase of $k_L a$ or the decrease of medium viscosity. In both fermentations, $k_L a$ decreases as exponential growth of the fungus occurs and reaches an asymptotic value once the stationary growth phase is reached. A helical impeller was employed successfully for rheological studies, avoiding problems of settling, jamming or pellet destruction, finding that the culture medium behaves as a pseudoplastic fluid. Rheological measurements were used to correlate gas holdup and $k_L a$ with apparent culture medium viscosity. Once again, for both fermentations, apparent viscosity increases as exponential growth of the fungus occurs and reaches an asymptotic value once the

stationary growth phase is reached. A satisfactory validation of experimental data for gas holdup and volumetric mass transfer coefficient was performed which allows to employ these data in scale-up strategies.

3. Case 2. Dynamic transport and reaction model for the removal of azo dye in a UAFB reactor

3.1 Introduction

Azo dye degradation from textile effluents has been the objective of research for some years due to the pollution problem they generate. For the removal of these compounds different processes have been applied: physicochemical, advanced oxidation, and biological. However there is a continuous search for an efficient, low cost and low environmental impact process to eliminate this problem. In particular, Reactive dyes are highly water soluble due to the sulphonated groups in their molecule so it cannot be reduced under the ordinary wastewater treatment processes (Beydilli, 2005). Anaerobic bioreactors have an important role in the treatment process of hazardous wastes, besides they can treat higher organic loads than aerobic reactors. Fixed bed reactors can be immerse, usually upflow, or trickle bed, downflow, the main characteristic is that the biomass is forming a biofilm covering a material that works as a support or carrier for the growth and maintenance of the microorganisms; in this way, the reactor efficiency is improved because the substrate-biomass contact is increased (effective surface area), and the process is more stable. The use of a carrier in the reactor is to improve the mechanical properties of the biomass and cell retention; in addition, the carrier may participate in the degradation process (Van der Zee, et al. 2003). A biofilm usually do not grow in a homogeneous way on the support, but rather forms clusters on the surface; the way in which a biofilm is grown and their internal structure is formed depends on the superficial velocity of the flow through the reactor, it is also affected by the mass transfer velocity and microorganism activity (Beyenal, 2002). The degree of biomass buildup affects the hydrodynamic behavior of the reactor. In this work, an Upflow Anaerobic Fixed Bed (UAFB) bioreactor with activated carbon (AC) as the carrier was used to remove azo dye from the effluent. It has been proved that AC possess good properties for biofilm growth and to remove diverse pollutants (Fan, et al. 1987; Fan, et al. 1990; Herzberg and Dosoretz, 2003; McCarty and Meyer,2005), moreover, AC could accelerate azo dye degradation due to its redox mediator function through the chemical groups on its surface (Van der Zee, et al. 2003) Di Iaconi et al (2005) proposed a mechanism for biofilm growth: 1) formation of a thin film covering the support by the microorganisms, 2) increment of the biofilm thickness, 3) the break of the added biofilm clusters and release of particles (biomass due to the excess of growth) and 4) small pellet formation by detached particles. In UAFB reactors it is common to have the bioparticles (carrier plus biofilm), some free cells and biomass pellets as a function of the superficial velocity on the reactor; the water flowing through the bioreactor can carry out the drag of small biomass pellets. The mass transport through this bioparticles occurs on three stages: diffusion of the dye molecule from the solution to the biofilm, diffusion through the biofilm, adsorption-diffusion through the carbon surface and reaction. One disadvantage of using upflow fixed bed reactors is that the liquid flow is non-ideal and dispersion, backmixing and bypassing flow are considerable (Iliuta, et al. 1996), therefore it is important to carry out the hydraulic characterization of the reactor through tracer test, although it is common to consider plug flow to model the reactor. The reasons of modelling a reactor of this kind are to estimate all the important parameters in its function, to optimize the efficiency and to predict its behaviour, besides its future scale-up. However, scaling a reactor from laboratory models is

often difficult, since some factors which are negligible when modelling small reactors have to be included in real reactor models, such as the transport between static and dynamic zones. Therefore, the main objective of this paper is to propose a dynamic mathematical model for an UAFB bioreactor with AC as carrier, to attach microorganisms and enhance biodegradation, in the removal of the azo dye reactive red 272 (Fig. 1).
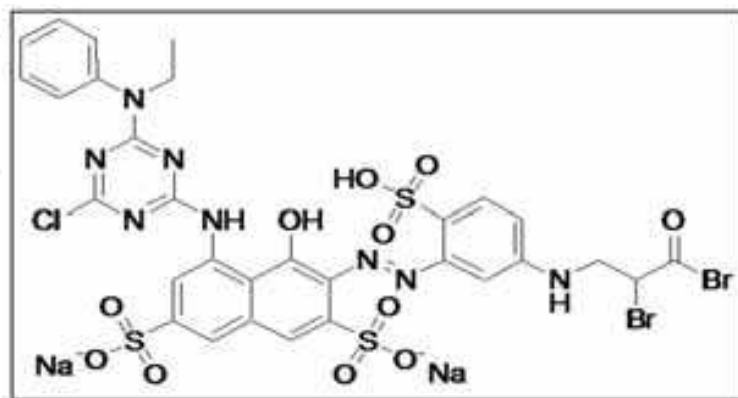

Fig. 1. Reactive red 272

The presented mathematical model includes all the transport phenomena: convection, dispersion, diffusion and mass transfer from one phase to another, along the reactor and through the bioparticle, as well as the reaction of dye reduction. The balance equations are coupled and solve together as a system. We try to include in the model all the possible phenomena that take place in the reactor in order to describe it and obtain enough information about it.

3.2 Materials and methods
3.2.1 Reactor assembling.

It was started up to work an anaerobic upflow reactor of the kind of the UAFB, made from Pyrex glass, with a fixed bed of AC of 42% of its operation volume, equivalent to 1.244 L and 541.17 g of AC. The reactor is outlined in Figure 2 and its characteristics are shown in Table 1.
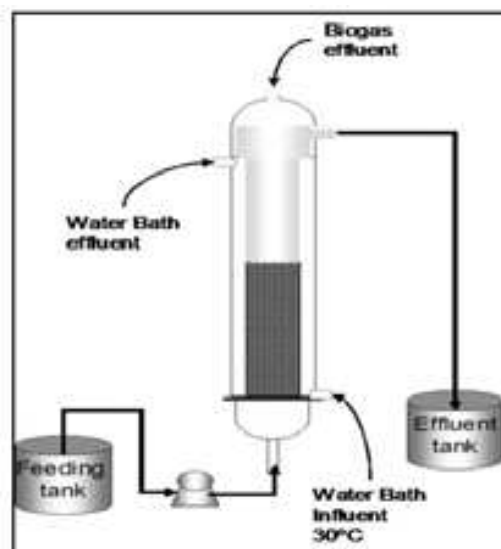

Fig. 2. Upflow Anaerobic Fixed Bed (UAFB) Reactor.

Work volume, L	3.3
Inside diameter, cm	6
Inside diameter of the settle, cm	9.5
Total longitude, cm	105.5
Initial and steady state porosity of the bed	0.53, 0.19
Fixed bed volume, L	1.244
Fixed bed longitude, cm	48
Superficial velocity (average), cm/min	0.52
Volumetric flow (average), mL/min	18
RT_m (average), min	206.25

Table 1. UAFB Reactor Characteristics

At the beginning, there was an adsorption stage to saturate the AC in the reactor with dye and do not attribute the removal efficiency to simply adsorption on to AC. Afterwards, the rector was inoculated by recirculating water with 10% v/v of adapted sludge for a period of 15 days; this was a consortium of microorganisms adapted to azo dye reduction using textile wastewater enriched with reactive red 272. In this stage, 11.586 mg biomass/g AC was adsorbed, forming a biofilm on the AC surface. The reactor was operated using synthetic wastewater, containing different azo dye concentration, from 100 to 500 mg/L, and 1 g/L of dextrose and yeast extract as carbon and nitrogen source to the microorganism.

3.2.2 Residence time distribution.

A lithium chloride solution was used as a tracer in order to determine the hydraulic characteristics of the reactor and to obtain the residence time distribution. Smith and Elliot (1996) used LiCl as a tracer and recommend a concentration of 5 mg Li+/L to avoid toxicity problems. In this case it was applied a one minute pulse of a 2000 mg/L LiCl solution. Dextrose and yeast extract with a concentration of 1 g/L were used as the substrates during the test. Samples were taken in the reactor effluent every 30 min during approximately 3 times the half residence time (RT_m), in this case, during 10 hr. Lithium concentration was analyzed in an atomic adsorption spectrophotometer (Perkin Elmer model 2280; USA).
The hydraulic residence time (HRT) was calculated as:

$$HRT = \frac{\int_0^\infty t(C - C_0)dt}{\int_0^\infty (C - C_0)dt} \tag{1}$$

Were C is the tracer concentration at a time t and C_0 is the tracer concentration at $t=0$. The parameters and non-dimensional numbers necessary to describe the reactor as well as the axial dispersion and mass transfer coefficients were calculated according to the next equations.
Dispersion number (d) and Péclet (Pe). These numbers indicate the dispersion grade in the reactor. A Pe above 1 indicates that convection is the leading factor in the mass transport, and if it is lesser than 1, the leading factor is the dispersion. The numbers are calculated as (Levenspiel, 2004):

$$d = \frac{1}{2}\frac{\sigma_{\Delta C}^2}{RT_m{}^2} = \frac{D}{uL} \tag{2}$$

$$Pe = \frac{uL}{D} = \frac{1}{d} \tag{3}$$

Where u is the superficial velocity in the reactor, L is the longitude and D is the axial dispersion coefficient.

Dispersion coefficient (D). It can be calculated by the dispersion number or by other correlations as the presented through the Reynolds number.

$$D = d\,u\,L = 1.01\nu\,N_{Re}^{0.875} \tag{4}$$

Here, ν is the cinematic viscosity of the water in the reactor (Levenspiel, 2004).

Sherwood number (Sh) and mass transfer coefficient (k$_m$). It was calculated by the Frössling correlation (Fogler, 1999), which is applied to the mass transfer or flux around a spherical

$$Sh = 2 + 0.6 N_{Re}^{1/2} Sc^{1/3} \tag{5}$$

particle. Supposing this the following equation was used:

And the mass transfer coefficient of the dye was estimated by the equation:

Where d_p is the average particle diameter of the carbon particles and biomass in the bed. For this analysis it was taken the d_p values of the carbon particles at the beginning of the study, 1.03 mm.

$$k_m = \frac{D_{ef}Sh}{d_P} \tag{6}$$

3.2.3 Kinetic model

The applied kinetic model to represent the dye biodegradation (reduction) was derived according to experimental observations, after fitting kinetic data at dye concentrations from 100 to 500 mg/l. The model expresses a change in the reaction order since it was noticed that the reaction in the system is a function of dye concentration and occur in two stages: first order, the dye is adsorbed by the bioparticle and reduced, and second, the enzymatic reactions take place to degrade the dye to certain extent. This is shown by Equation 7, here: C_{A0} and C_A are the initial and every moment dye concentration, k_1 and k_2 are 1st and 2nd order specific reaction rate, (h^{-1}, L/mg·h). The deduction is explained in another paper (in revision).

$$r_A = -\frac{dC_A}{dt} = k_1 C_A - k_2 C_A (C_{A_0} - C_A) \tag{7}$$

3.2.4 Model dimensionless numbers

From the dimensionless analysis of the model, the dimensionless numbers that explain the transport process in the reactor were obtained. These were: Biot's number (Bi), that relates mass transfer with diffusivity, Fourier's number (Fo), that relates the diffusivity in the reaction area in the reaction time, Wagner's module (Φ^2), by means of which it is obtained the Thiele's number (Φ) that indicates if diffusion modifies the reaction rate; from this number, the Effectiveness factor (η) is calculated, which relates the real reaction rate with the reaction rate without diffusion resistance, in other words, it expresses the influence of

the diffusion on the reaction rate. Thiele number is calculated by Equation 8 (according the proposed kinetic model there is a Thiele number for the first order term and other for the second order term). The Effectiveness factor for the reduction rate of the dye by volume unit of bioparticle was calculated using Equation 9, according to the definition of volume average (Escamilla-Silva et al, 2001) and using the proposed kinetic model expressed in Equation 7. Here, $\overline{R_A}$ is the average reaction rate in the biofilm and $R_A\big|_{\xi=1}$ is the reaction rate in the bioparticle surface in the liquid boundary; Fo_b is the characteristic Fourier number for the biofilm defined in Equation 19, in the next section.

$$\Phi_1 = \delta\sqrt{\frac{k_1}{D_{eb}}} \;\; ; \;\; \Phi_2 = \delta\sqrt{\frac{k_2 C_{A0}}{D_{eb}}} \tag{8}$$

$$\eta = \frac{4\pi\int_0^1 R_A \xi^2 d\xi}{\frac{4}{3}\pi R_A\big|_{\xi=1}} = \frac{3\int_0^1 R_A \xi^2 d\xi}{R_A\big|_{\xi=1}} = \frac{3\int_0^1\left[\Phi_1^2 Fo_b\omega_b - \Phi_2^2 Fo_b\omega_b(\omega_L - \omega_b)\right]\xi^2 d\xi}{\left[\Phi_1^2 Fo_b\omega_b - \Phi_2^2 Fo_b\omega_b(\omega_L - \omega_b)\right]\big|_{\xi=1}} = \frac{\overline{R_A}}{R_A\big|_{\xi=1}} \tag{9}$$

3.3 Results and discussion.

The UAFB reactor efficiently removes the reactive red dye, from 91.35% to 98.64% and up to 56% of DQO, at inflow concentration from 100 to 500 mg/L and at a RT_m from 3 to 5 hours. Higher removal rates can be obtained at higher residence times. The difference between colour and COD removal is because the first step in the biodegradation of the dye takes place when the azo bond is broken, and this results in the lost of colour of the solution. There are aromatics amines and other organic compounds in the water as products of dye reduction, which can be degraded to a certain extent in to other low molecular weight molecules, as carboxylic acids. The results described in this section are in regard to an analysis of the transport and reaction phenomena inside the reactor and to obtain predictions about its performance. The balance equations are proposed according to theoretical principles. Some of the parameters used were calculated according to experimental and real results and others in base to references. The model can be used and applied to similar problems, but it will need a parameter fit. Because of this, the real removal rate of the reactor is higher than the predicted for the model, at the highest dye concentration used (400-500 mg/L).

3.4 Residence time distribution.

The parameters and non-dimensional numbers that describe the transport in the reactor fixed bed are shown in Table 1. The superficial velocity was calculated as $u_L = Q/\varepsilon_L \pi R_i^2$ and the porosity of the bed ε_L was 0.19 after equilibrium was reached. The hydraulic behaviour of the reactor was approximated to a plug flow with axial dispersion. Figure 3 show HRT distribution curves; it was observed that when Q was increased, the dispersion was reduced and the reactor was closer to ideal plug flow behaviour. This is a hydrodynamic effect, but for packed beds it is attributed to the particle size of the packing material. This result can be attributed to the fine particles formed with time operation in the inter-particle space in the reactor, because it reduces the bed porosity and as a result the by-pass fluxes. Kulkarni et al (Kulkarni, 2005) established that the fine particles formed in packed bed reactors reduce the by-pass flux because there is a better spreading of the water flow, and therefore the

dispersion is reduced. During the residence time distribution tests there was biogas production due to the digestion of dextrose in the synthetic wastewater, however, the biogas production with or without dye in the water is not enough to consider the reactor as a mixed tank. Besides, the rise of biogas through the bed is very slow, this generates by-pass flow due to the biogas bubbles trapped, and when the superficial velocity in the reactor is increased, the bubbles are pushed and can flow better and the by-pass flux is reduced; thus the reactor became closer to a plug flow. The HRT was from 1.6 to 1.8 times the RT_m at the less volumetric flow in the reactor, and from 1.1 to 1.3 times at high volumetric flow. The residence time distribution achieved for all the tests was fitted by a statistical distribution of extreme value (Fisher-Tippet) shown by Equation 10; this is a frequency distribution function for slant peaks.

$$P(t) = y_0 + a * Exp\left[-Exp(-f1) - f1 * s + 1\right]$$
$$f1 = \frac{t - t_C}{w} \tag{10}$$

Where $P(t)$ is the normalized tracer concentration, y_0 represents the distribution displacement (time 0 tracer concentration), a is the amplitude of the distribution and w the wide of the peak. These calculated parameters, the error and correlation coefficient ($p<5$). Figure 3 shows the residence time distribution in the reactor for each test and the fit by the Extreme model. Iliuta et al (1996), states that a long tail in the residence time distribution could be caused because of axial dispersion in the dynamic flow as well as the mass transfer between the dynamic and static zones. Also, when the reactor has porous particles in the packed bed, as in this case, the alteration in the distribution can be attributed to internal diffusion and reversible adsorption of the tracer, however, this is negligible, but it happens for the dye.

The reactive red 272 dye molecule is adsorbed reversible and superficially on to biomass, also is adsorbed onto AC surface, but poorly, and has a limited adsorption capacity due to its molecule size and chemical groups as naphthalene disulphonic acid, a choloro-triazine and phenyl-amine (see Fig. 1); also AC has limited active sites for adsorption. There is an equilibrium between adsorption, reaction and desorption. In this case it is considered a constant saturation of the bioparticle, so the adsorption dynamics will be negligible.
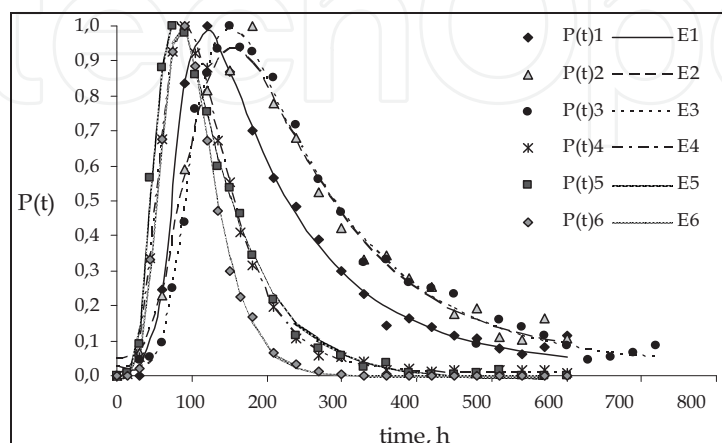

Fig. 3. HRT distribution; tracer pulse applied to the bioreactor.

Parameter	HRT1	HRT2	HRT3	HRT4	HRT5	HRT6
RT_m (min)	57.264	66.203	66.203	42.412	42.412	42.412
u_L (cm/s)	0.0735	0.0631	0.0631	0.0985	0.0985	0.0985
N_{ReL}	54.962	47.468	47.468	74.096	74.096	74.096
Bo_L	11029.2	9461.54	9461.54	14769.2	14769.2	14769.2
d_L	2.864	2.255	2.407	2.332	1.208	0.413
D_L (cm^2/s)	10.026	6.828	7.287	11.022	5.709	1.953
Pe_L	0.349	0.443	0.415	0.429	0.828	2.420
Sh_L	45.403	42.246	42.246	52.283	52.283	52.283
k_L (cm/s)	0.0176	0.0164	0.0164	0.0203	0.0203	0.0203
y_0	0.0270	0.0470	0.0251	7.6×10^{-3}	9.3×10^{-3}	5.5×10^{-4}
a	0.5697	0.6629	0.6175	0.8944	0.6959	1.0029
w	22.033	46.312	33.212	29.893	19.756	32.259
SE[a]	0.0255	0.0443	0.0325	0.0182	0.0226	0.0162
R^2 [b]	0.9945	0.9823	0.9920	0.9977	0.9966	0.9980

Table 2. Hidrodinamic, mass transfer and and fitted extreme
model Parameters for the UAFB reactor (L = fixed bed).

3.5 Dynamic model: Transport and reaction in the fixed bed

After the calculus of HRT and all the necessary parameters and dimensionless numbers, a mathematical model was deduced and executed to represent the transport and reaction of the dye in the water upflow through the reactor (the clarifier zone is not considered here due to complexity of the process).

The dynamic model is based in the next assumptions:

1. Radial dispersion is negligible.
2. The reactor is divided in two zones: the fixed bed and the clarifier (not considered) and there is mass transfer between them.
3. The dispersion coefficient is constant in each zone.
4. There is mass transfer between the water flowing through the bed and the bioparticles.
5. The superficial velocity trough the bed is constant and calculated as $u_L = Q / \varepsilon_L \pi R_i^2$.
6. The dye can be reversible adsorbed into bioparticles.
7. The dye is diffused, adsorbed and reacts in the biofilm and there is superficial diffusion in the activated carbon core macropores because the molecule size (21 Å) would limit the micropore diffusion (pore average diameter 23.3 Å).
8. The particle is spherical and with a uniform and porous biofilm.
9. The biomass on the activated carbon core grow up to certain thickness, and afterwards the biomass excess is detached and form small granules, then the biomass attached on the activated carbon came back to their normal or equilibrium thickness. Thus, there is a dynamic in the biofilm thickness but will be taken as an average value supposing equilibrium between grow and detachment. The model includes the balance in the bioparticle divided in two zones: zone I represents the AC particle (core) and zone II the microorganism biofilm surrounding the AC core. The reaction term is included in two balance equations, in the zone II of the bioparticle and in the liquid balance; this because is an extracellular process and there are free cells or small biomass granules in the flowing liquid. Figure 4 shows a graphical scheme of the model; here C_{AL} is the liquid concentration of the dye, C_{AP} is the dye concentration in the AC core, and C_{Ab} the biofilm concentration.
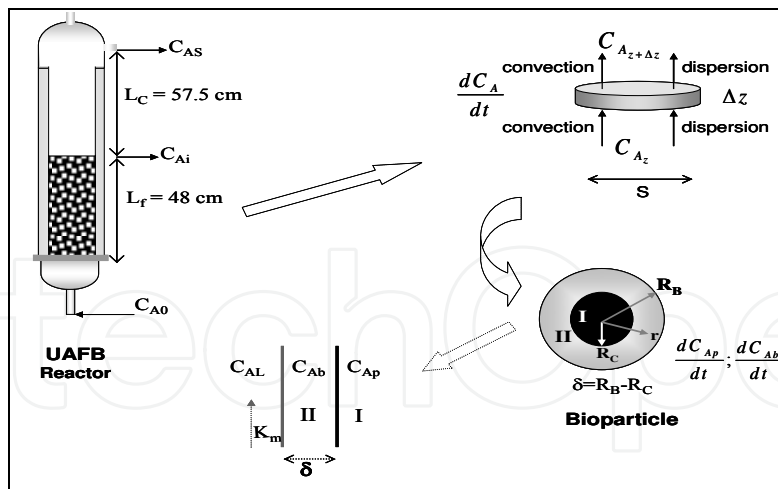
Fig. 4. Transport and reaction model in the UAFB, Reactor scheme.

The governing equations are:

a) **Balance for the liquid flow in the fixed bed.**

$$\frac{\partial C_{AL}}{\partial t} = D_L \frac{\partial^2 C_{AL}}{\partial Z^2} - u_L \frac{\partial C_{AL}}{\partial Z} - K_m a_{sb}(C_{AL} - C_{Ab}\big|_{r=R_B}) - k_1 C_{AL} + k_2 C_{AL}(C_{A0} - C_{AL}) \qquad (11)$$

This equation describes the dye convection, dispersion and mass transfer from the liquid phase to the biofilm surface and the reaction. The initial and boundary conditions are:

$$t = 0 \qquad C_{AL} = C_{A0}$$

$$Z = 0 \qquad C_{AL} = C_{A0} \qquad\qquad (12)$$

$$Z = L_f \qquad \frac{\partial C_{AL}}{\partial Z} = 0$$

b) **Balance for the bioparticle.**

For the AC core:

$$\frac{\partial C_{Ap}}{\partial t} = D_{ep}\left(\frac{2}{r}\frac{\partial C_{Ap}}{\partial r} + \frac{\partial^2 C_{Ap}}{\partial r^2} \right) \qquad\qquad (13)$$

This equation describes the dye convection and diffusion. The initial and boundary conditions that expresses field equality in the interface are:

$$t = 0 \qquad C_{Ap} = 0$$

$$r = 0 \qquad \frac{\partial C_{Ap}}{\partial r} = 0 \qquad\qquad (14)$$

$$r = R_C \qquad C_{Ap} = C_{Ab}$$

For the biofilm (diffusion and reaction):

$$\frac{\partial C_{Ab}}{\partial t} = D_{eb}\left(\frac{2}{r}\frac{\partial C_{Ab}}{\partial r} + \frac{\partial^2 C_{Ab}}{\partial r^2}\right) - k_1 C_{AL} + k_2 C_{AL}(C_{A0} - C_{AL}) \tag{15}$$

This equation describes the dye convection, diffusion and reaction. The initial and boundary conditions that expresses flux equality in the interface and mass transfer from the bioparticle to the liquid phase are:

$$t = 0 \qquad C_{Ab} = 0$$

$$r = R_C \quad -D_{ep}\frac{\partial C_{Ap}}{\partial r} = -D_{eb}\frac{\partial C_{Ab}}{\partial r} \tag{16}$$

$$r = R_B \quad -D_{eb}\frac{\partial C_{Ab}}{\partial r} = K_m\left(C_{Ab} - C_{AL}\right)$$

c) Dimensionless model. The dimensionless governing equations are shown next.

For the liquid flow in the fixed bed:

$$\frac{\partial \omega_L}{\partial \tau} = d_L\frac{\partial^2 \omega_L}{\partial \zeta^2} - \frac{\partial \omega_L}{\partial \zeta} - \beta_m(\omega_L - \omega_b) - \Phi_1^2 Fo_b\omega_L + \Phi_2^2 Fo_b\omega_L\left(1 - \omega_L\right) \tag{17}$$

$$\tau = 0 \qquad \omega_L = 1$$

$$\zeta = 0 \qquad \omega_L = 1 \tag{18}$$

$$\zeta = 1 \qquad \frac{\partial \omega_L}{\partial \varsigma} = 0$$

Using the dimensionless numbers:

$$\omega_L = \frac{C_{AL}}{C_{A0}} \quad ; \quad \zeta = \frac{Z}{L_f} \quad ; \quad \tau = \frac{t}{t_{mL}} = \frac{tu_L}{L_f} \quad ; \quad d_L = \frac{D_L}{u_L L_f} = \frac{1}{Pe_L} \quad ; \quad \beta_m = \frac{K_m a_{sb} L_f}{u_L}$$

$$\Phi_1^2 = \frac{\delta^2 k_1}{D_{eb}} \quad ; \quad \Phi_2^2 = \frac{\delta^2 k_2 C_{A0}}{D_{eb}} \quad ; \quad Fo_b = \frac{D_{eb} L_f}{\delta^2 u_L} \tag{19}$$

In order to become dimensionless the two zones of the bioparticle, it was proposed a parallel model; the AC core and the biofilm are then expressed as a single particle with a radius from 0 to 1 (see Fig. 5):

For the AC core:

$$\frac{\partial \omega_p}{\partial \tau} = Fo_p\left(\frac{2}{\xi}\frac{\partial \omega_p}{\partial \xi} + \frac{\partial^2 \omega_p}{\partial \xi^2}\right) \tag{20}$$

$$\tau = 0 \qquad \omega_p = 1$$

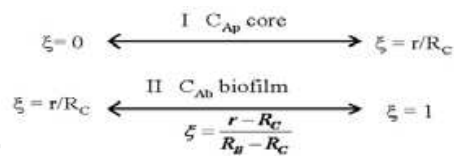$$\xi = 0 \tag{21}$$

$$\xi = 1 \quad \omega_p = \omega_b$$

Fig. 5. Parallel dimensionless model.

Using the dimensionless numbers:

$$\omega_p = \frac{C_{Ap}}{C_{A0}} \quad ; \quad Fo_p = \frac{D_{ep}L_f}{R_C^2 u_L} \quad ; \quad \tau = \frac{t}{t_{mL}} = \frac{t u_L}{L_f} \tag{22}$$

For the biofilm:

$$\frac{\partial \omega_b}{\partial \tau} = Fo_b \left[\frac{\partial^2 \omega_b}{\partial \xi^2} + \left(\frac{2}{\xi + \beta} \right) \frac{\partial \omega_b}{\partial \xi} \right] - \Phi_1^2 Fo_b \omega_b + \Phi_2^2 Fo_b \omega_b \left(\omega_L - \omega_b \right) \tag{23}$$

$$\tau = 0 \quad \omega_b = 0$$

$$\xi = 0 \quad \frac{\partial \omega_b}{\partial \xi} = \alpha \ \beta \frac{\partial \omega_p}{\partial \xi} \tag{24}$$

$$\xi = 1 \quad \frac{\partial \omega_b}{\partial \xi} + Bi \ \omega_b = Bi \ \omega_L$$

Using the dimensionless numbers:

$$\omega_b = \frac{C_{Ab}}{C_{A0}} \quad ; \quad \tau = \frac{t}{t_{mL}} = \frac{t u_L}{L_f} \quad ; \quad \Phi_1^2 = \frac{\delta^2 k_1}{D_{eb}} \quad ; \quad \Phi_2^2 = \frac{\delta^2 k_2 C_{A0}}{D_{eb}} \quad ; \quad Fo_b = \frac{D_{eb}L_f}{\delta^2 u_L}$$

$$Bi = \frac{K_m R_B}{D_{eb}} \quad ; \quad \alpha = \frac{D_{eb}}{D_{ep}} \quad ; \quad \beta = \frac{R_C}{R_B - R_C} = \frac{R_C}{\delta} \tag{25}$$

The reactor model then consist of three differential parabolic equations; to solve the model, all the parameters are calculated and is used the finite differences with a 5th order Runge-Kutta-Fehlberg method, programmed in Fortran language.

3.6 Model solution.

The data that we had previous to the model solving are: from the AC properties: $\rho_p = 0.435$ g/cm³ (density), $\varepsilon_p = 0.1392$ (porosity), $R_C = 0.0515$ cm (average particle radius), and about the reactor we have: $L_L = 48$ cm (longitude), $R_i = 3$ cm (radius), $\varepsilon_L = 0.19$ (bed porosity). The dispersion coefficient (D_L), the dispersion number (d_L), the Peclet number (Pe), the superficial velocity (u_L) and the half residence time (RT_m), were estimated in the residence

time distribution analysis, as was explained in the methodology section. The diffusion coefficient in the AC core was calculated by the method explained in Hines and Hines and Maddox (1987), supposing Knudsen diffusivity, but the value was changed in two orders of magnitud in order to fit the model (Fan et al. 1990; Lee et al.2006), comparing the values reported for other dyes in references. The diffusivity in the biofilm was assumed to be 100 times larger than the diffusivity in the AC core, based in values reported for other dyes of the same kind (Fan et al. 1987; Chen et al. 2003). The kinetic constants were estimated from experimental data and fitted to model.

The mass transfer surface of the bioparticles was calculated by the Equation 20 proposed by Iliuta and Larachi (2005)

$$a_{sb} = \frac{6}{d_b} = \frac{6}{d_p + 2\gamma} \qquad (26)$$

The parameters used to solve the mathematical model are shown in Table 4; in this case, the Thiele number of second order is applied for an initial dye concentration of 250 mg/L, for 400 mg/L was 1.43 and for 500 mg/L was 1.60. This indicates that when the dye concentration is augmented in the reactor influent, the mass transfer effects are increased, specifically the resistance to the diffusion, and therefore, it decreases dye removal. Figure 6 shows the concentration profile along the reactor to different dye concentration at the reactor inflow, and Figure 7 shows the concentration profile within the bioparticle (AC core plus biofilm) for an initial concentration of 250 mg/L.

It can be seen in the Figure 7 that the particles close to the reactor influent ($\zeta = 0.045$) contain higher dye concentration than the ones in the effluent extreme, whose concentration is close to the dye effluent concentration. The concentration profile in the bioparticle changes with time as the bioparticle is saturated and reaches equilibrium, while a curve indicative of the reaction in the biofilm is observed. When the bioparticle is close to the effluent, the profile is becoming flat, and the concentration is approximately uniform within the bioparticle. This is because at the effluent zone there is the smallest dye concentration in the reactor height, and the kinetics depends on this.
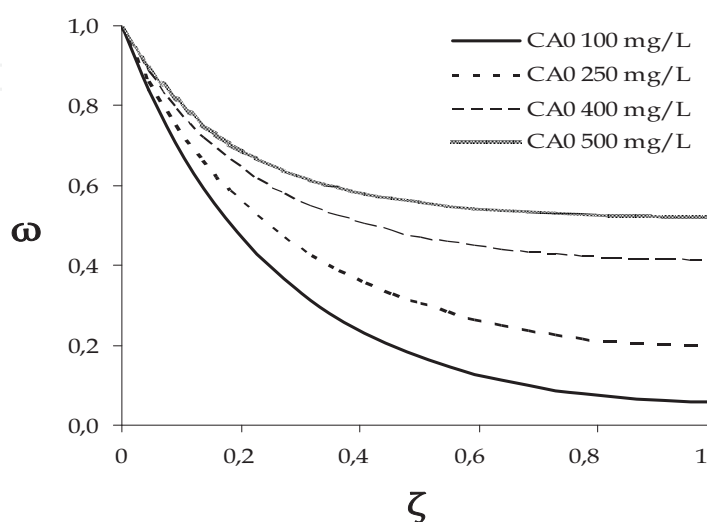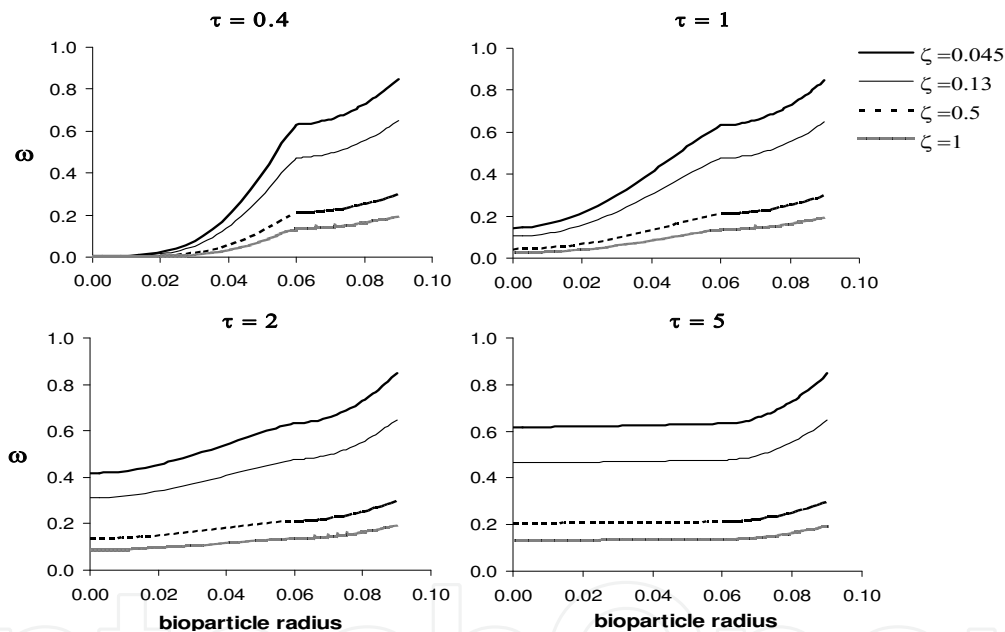

Fig. 6. Predicted concentration profile along the reactor

D_L	(cm^2/min)	423.4	Φ_1^2 [a]	1.061
u	(cm/min)	3.786	Φ_2^2 [b]	1.276
K_m	(cm/min)	0.984	Φ_1 [c]	1.030
D_{ep}	(cm^2/min)	2.58×10^{-5}	Φ_2 [d]	1.130
D_{eb}	(cm^2/min)	2.58×10^{-3}	β	2
k_1	(min^{-1})	3.046	α	100
k_2	$(L/mg\cdot min)$	1.47×10^{-2}	Bi	34.27
a_{sb}	(cm^2/cm^3)	36.81	B_m	459.22
F_{op}		0.091	d_L	2.33
F_{ob}		36.404		

Table 4. Parameters used in model solution.

Fig. 7. Predicted concentration profile in the bioparticle at different τ and ζ in the bed. Radius in cm.

The RT_m in the reactor does not have much influence on the removal of the dye according the predicted results of the model. Figure 8 shows the concentration profile along the reactor at different conditions of RT_m (See Tab. 3), and using a dye inflow concentration of 250 mg/L; it can be seen that there is not a noticeable effect in the concentration profile as RT_m is incremented. The concentration profile in the bioparticle is affected in a different way by the RT_m; in Figure 9 we can see that as RT_m is increased, the bioparticles are saturated faster, this is because the contact time for adsorption and for reaction is augmented and the mass transfer between the liquid phase and the bioparticles is improved.

As a result, the RT_m in the reactor affects only the mass transport rate in the reactor but not the biodegradation reaction and thus does not have an influence on the concentration profile along the reactor and consequently, in the removal efficiency. Therefore, analyzing the

profiles expressed in Figure 6, the main factor that affects the removal efficiency is the inflow dye concentration.

Similar results were found by other authors. Spigno et al (2004) presented a mathematical model for the steady state degradation of phenol along a biofilter reactor and obtained a concentration profile for phenol reduction at two different concentrations, and they found the same profile for both conditions displaced by a concentration gradient, more reduction at the lesser concentration. Mammarella and Rubiolo (2006) could predict the concentration profile for lactose hydrolysis in an immobilized enzyme packed bed reactor under different operation conditions, and they obtained an asymptotic profile for lactose conversion along the reactor height and obtained a much higher conversion at the lesser volumetric flow (100 mL/h); on the contrary, in this work the volumetric flow does not have much influence. These authors did not include the dynamic of the pollutant inside the bioparticle, as is shown in this work.
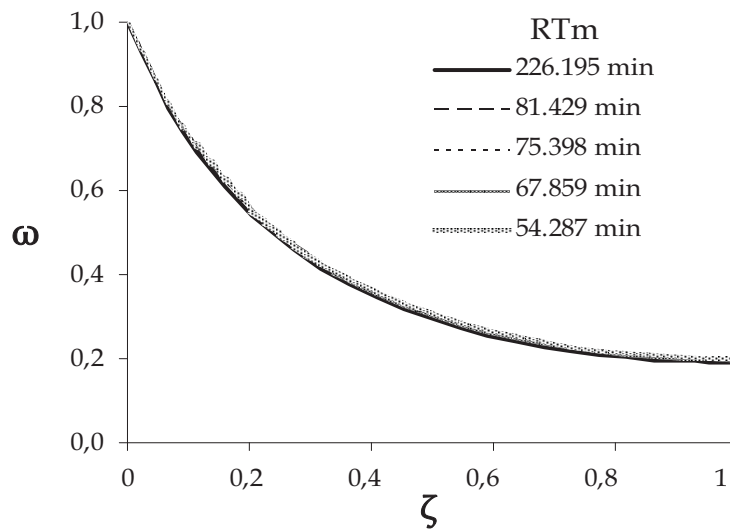

Fig. 8. Predicted concentration profile along the reactor a different RT_m

RT_m (min)	226.195	81.429	75.398	67.859	54.287
Q (cm³/min)	6.000	16.67	18.00	20.00	25.00
u (cm/min)	1.117	3.102	3.351	3.723	4.654
K_m (cm/min)	0.695	0.913	0.939	0.978	1.083
d_L	7.899	2.843	2.633	2.370	1.896
β_m	1099.8	519.7	495.1	464.4	411.5
F_{op}	0.308	0.111	0.103	0.093	0.074
F_{ob}	123.4	44.42	41.13	37.02	29.62
Bi	24.21	31.78	32.70	34.07	37.75

Table 5. Parameters used in model solution at different RT_m

Leitão and Rodrigues (1996) presented the influence of the biofilm thickness on the removal of a substrate when the support carrier material is an adsorbent and when it is not, and they obtained the concentration profile within the bioparticle but in the absence of reaction; the profiles show the saturation of the bioparticle as time increases, and the concentration augments as the biofilm thickness increase, but it was not observed the reaction zone in the biofilm as in the results presented in this work. Leitão and Rodrigues (1998) proposed an intraparticle model for biofilms on to a carrier material including the convective flow inside the particle, and they obtained the concentration profile and biofilm thickness regarding time. They conclude that bioreactors have to be operated under conditions such that allow the liquid movement to occur in the void space of the biofilm, in order to improve mass transfer and as a result the efficiency of the process.
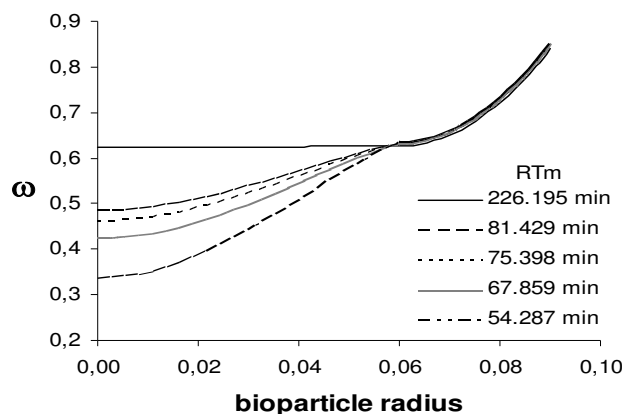

Fig. 9. Predicted concentration profile in the bioparticle at different RT_m.
Radius in cm.$\tau = 2$ and $\zeta = 0.045$ (close to the influent) in the bed.

In biofilms the hydrodynamics and kinetics of the system is related to the fact that most biofilm reactions are diffusion limited, therefore the shape of the concentration profiles will be determined by diffusivity and convection (Lewandowski, 1994). We suppose that the biofilm is a continuous phase, but it is not, biofilms are formed by clusters, void spaces and channels, so the convection in the system is important, and the measured diffusion coefficients are always approximations. The effect of convection in the bioparticle is shown in Figure 9; mass transfer in the biofilm is fast but in the core the RT_m affects the mass transfer and as a result the concentration profile.
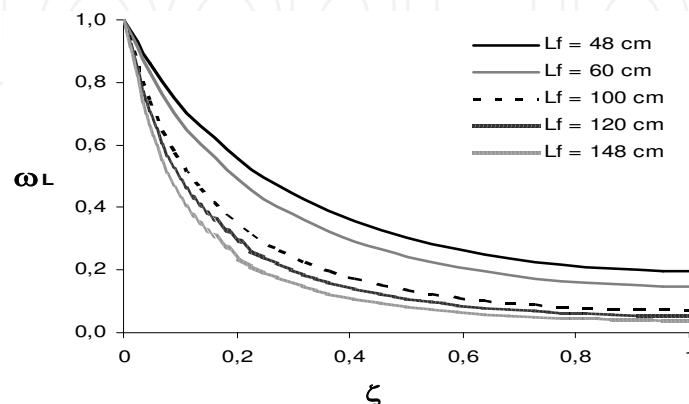

Fig. 10. Predicted concentration profile along the reactor, increasing the reactor bed height (L_f). $C_{A0} = 250$ mg/L at the inlet.

The effect of the bed height is shown in Figure 10, with a constant inlet dye concentration of 250 mg/L. Here we can see that the dimensionless dye concentration is reduced as the longitude of the bed height (L_f) is increased, this means higher removal efficiency; a higher L_f implies more bioparticles and time for degradation reaction, however the most of the reduction of the dye is carried out in the lower third of the bed longitude.

3.7 Effectiveness factor.
The effectiveness factor (η) was calculated at different azo dye concentration at the reactor influent, from 100 to 500 mg/L, and at different RT_m from 54.3 to 226.2 min. Each calculation was carried out taking the predicted dimensionless concentration value in the biofilm and in the liquid, and solving the model for a $\tau = 2$. The results explain that the average reaction rate in the biofilm and at the biofilm surface is changed regarding the height of the reactor, and in consequence the effectiveness factor; furthermore, the effectiveness factor depends mainly on the azo dye concentration. The change of the reaction rate regarding the reactor height is explained because there is a higher amount of active biomass at the inlet, at the bottom of the reactor. In this zone, dye and substrate concentration (dextrose and yeast extract) is always higher and in consequence there is always a major reaction activity; therefore, in this zone takes place the most of the degradation of the dye, as it was also noticed in Figure 6. The calculated effectiveness factor decreased from 0.78 to 0.47 when dye concentration was increased from 100 to 500 mg/l, proving that, when dye concentration is increased the diffusion of dye through biofilm has a major influence on the reaction rate, what is reflected in a reduction of the efficiency of removal. On the contrary, changes in RT_m in the reactor at a constant inflow dye concentration did not influence the value of the effectiveness factor; this did vary from 0.74 to 0.73 when RT_m was decreased from 226.2 to 54.3 min. These values indicate that there is a slight effect of dye diffusion on the reaction rate when RT_m is changed.

3.8 Conclusions
The proposed mathematical model for a UAFB bioreactor was able to predict the concentration profiles along the reactor and within the bioparticle (carbon core and biofilm) for the biodegradation of a reactive red azo dye, using a kinetic model with a change in reaction order. The profiles at different inflow dye concentration showed an asymptotic curve with a major activity of reaction in the lower zone of the reactor, and this concentration fall is reduced as the inflow dye concentration is augmented. Nevertheless, the RT_m does not have much influence on the concentration profile along the reactor. In addition, the model predicts a larger removal rate as the longitude of the bed is increased for the same inlet dye concentration.
The profiles within the bioparticle illustrate the saturation of the particle and reflect the zone of reaction in the biofilm; it can be seen the differences in the concentration values with regard to the reaction zone along the reactor. The saturation rate of the bioparticles change with the RT_m, at a larger time, the mass transfer is improved and the bioparticles are saturated faster, without affecting the reaction. The calculation of the effectiveness factor showed that the rate of reaction is changed in regard to the position at the height of the reactor and depends of the dye diffusion when the concentration is increased. By means of the presented dynamic model it can be predicted the dye and COD removal rate in a UAFB reactor, specifying its characteristics, dye inflow concentration, and residence time.

3.9 Nomenclature

a_{sb}	Specific surface of the particles, cm^2/cm^3
C, C_A	Dye or tracer concentration, mg/L
C_0, C_{A0}	Initial tracer, dye concentration, mg/L
C_m	Average concentration, mg/L
d	Dispersion number
D	Axial dispersion coefficient, cm^2/s
D_e	Effective diffusivity coefficient, cm^2/s
K_m	Mass transfer coefficient, cm/s
k_1	1st order specific reaction rate, h^{-1}
k_2	2nd order specific reaction rate, $L/mg·h$
L_f	Reactor bed height, cm
Q	Volumetric flow
r_A	Reaction rate, $mg/L·h$
R_B	Bioparticle radius, cm
R_C	AC core radius, cm
R_i	Reactor internal radius, cm
S	Crosswise area to the flux, cm^2
HRT	Hydraulic residence time
t	Time
t_m, RT_m	Half residence time
V_P	Pore volume
u	Superficial velocity
ρ	Density, g/cm^3
ε	Porosity
δ	Biofilm thickness
ζ	Dimensionless longitude
ξ	Dimensionless particle radius
ω	Dimensionless concentration
τ	Dimensionless time
Fo	Characteristic Fourier number
Bi	Biot number
Φ^2	Wagner number
Φ	Thiele number
βm	Dimensionless parameter
α	Dimensionless parameter
β	Dimensionless parameter

Subindex

b	biofilm
L	fixed bed
p	AC particle
1	For the first order term
2	For the second order term

4. Case III. A method to evaluate the isothermal effectiveness factor for dynamic of oxygen in mycelial pellets in submerged cultures

4.1 Introduction

Although a lot of research has been done into modelling microbial processes, the applicability of these concepts to problems specific for bioreactor design and optimization of process conditions is limited. This is partly due to the tendency to separate the two essential factors of bioreactor modelling, i.e. physical transport processes and microbial kinetics. The deficiencies of these models become especially evident in industrial production processes where O_2 supply is likely to become the limiting factor, e.g. production of gibberellic acid and other organic acids (Takamatsu et al. 1981; Qian et al. 1994; Lu et al. 1995; Hollmann,et al.1995). Important physical transport processes related to O_2 supply have not always received sufficient attention (el-Enshasy et al. 1999; Yamane and Shimizu, 1984; Wang and Stephanopoulos, 1984; Parulekar and Lim 1985; Sharon et al. 1999; Stephanopoulos and Tsiveriotis, 1989). Attempts to obtain optimal trajectories for various control variables in different bioreactors, in particular at different scale of operation, are likely to cause unrealistic conditions far from the expected optimum. Another reason to combine the intrinsic O_2 kinetics for growth and product formation with mass transfer is related to O_2 gradients on production scale. Recent attempts to account for these effects in stirrer bioreactors use different structured models and include the O_2 supply in viscous mycelial fermentation broths (Reuss et al. 1986; Nielsen and Villadsen, 1994; Sunil and Subhash, 1996; Cui et al. 1998; Goosen, 1999; Fan et al.1996). It is important when evaluating the potential of a fermentation process using mycelial pellets to have a mathematical model that can predict the O_2 consumption, fungal growth rates and substrate consumption.

In this study, we present a model that combines transport phenomena and kinetic mechanisms for O_2 consumption and applied it to a process in which gibberellin was produced in a submerged fermentation with mycelia of *Gibberella fujikuroi*. The effectiveness factors found in this work are compared to those reported in literature for other fungi.

4.2 Mathematical modelling

The mathematical model was developed assuming a bioreactor in which the continuous phase was well mixed and experimentally verified. O_2 concentration in the bioreactor was measured so the model only considered O_2 transport in the pellets. The method of volume-averaging was used to simulate bulk transport in a two-phase system (Carbonell and Whitaker, 1984; Ochoa, 1986):

$$\frac{\partial C}{\partial t} + \nabla.(\mathbf{v}C) = \mathbf{D} : \nabla\nabla C + k_o \rho \qquad (1)$$

with C the dissolved O_2 concentration (kg-moles O_2 m^{-3}), t time (h), k_o the specific O_2 uptake rate per unit dry mycelial weight (kg-moles O_2 kg^{-1} of dry cell h^{-1}) and ρ the pellet suspension density (kg m^{-3}).

The use of average transport equations imposes constraints on the length and physicochemical parameters of the system (Whitaker, 1991). The following assumptions were made to model the O_2 diffusion and reaction in the pellets:

1. The pellet is an effective system, isotropic with constant thermodynamic properties. Effective diffusivity of O_2 in porous medium can be used and the scalar D_{eff} or the effective diffusivity coefficient of dissolved O_2 in mycelial pellet (m^2 h^{-1}) replaces the tensor **D** of eq 1. Effective diffusivity contains the convective effects generated inside the pellets.
    1.03 mm.
2. D_{eff} is only a function of void fraction as proposed by different authors (e.g. Aris, 1975).
3. Mycelial pellets are spherical, and the O_2 transport occurs only in the radial direction.
4. An analogous Michaelis-Menten model was used to describe the O_2 consumption rate:

$$k_o = \frac{(k_o)_{max} C}{K_m + C} \tag{2}$$

where $(k_o)_{max}$ is the maximum specific O_2 uptake rate per unit dry mycelial weight (kg-moles O_2 kg^{-1} of dry cell h^{-1}) and K_m the apparent Michaelis constant for mycelia (kg-moles m^{-3}) and the transport equation (eq 1) can be reduced to :

$$\frac{\partial C}{\partial t} = D_{eff} \left[\frac{1}{r^2} \frac{\partial}{\partial r} \left(r^2 \frac{\partial C}{\partial r} \right) \right] - k_o \rho \tag{3}$$

with r the radial distance from the centre of the mycelial pellet (m). Boundary conditions for eq 3 were:

$$1 \quad @ \quad r = R \quad -D_{eff} \frac{\partial C}{\partial r} = k_P(C_S - C_L) \quad t>0 \tag{4a}$$

$$2 \quad @ \quad r=0 \quad \frac{\partial C}{\partial r} = 0 \quad t>0 \tag{4b}$$

with R the radius of the mycelial pellet (m), k_P the mass-transfer coefficient for the liquid film around cells or pellets (m h^{-1}), C_L the concentration of dissolved O_2 in bulk of liquid (kg-moles O_2 m^{-3}) and C_S the concentration of dissolved O_2 at the liquid-pellet interface (kg-moles O_2 m^{-3}).
Initial conditions were:

$$t = 0 \quad C = C_o \quad 0 \leq r \leq R \tag{5}$$

with C_O the initial concentration of dissolved O_2 (kg mole O_2 m^{-3}).
The dissolved O_2 concentration was monitored during the fermentation and is expressed as:

$$C_L = C_o f(t).$$

Using the dimensionless variables:

$$u = \frac{C}{C_o} \quad \xi = \frac{r}{R} \quad \tau = \frac{D_{eff} t}{R^2} \tag{6}$$

and introducing them into eqs 3 to 5 gives the dimensionless boundary value problem:

$$\frac{\partial u}{\partial \tau} = \frac{1}{\xi^2}\frac{\partial}{\partial \xi}\left(\xi^2 \frac{\partial u}{\partial \xi}\right) - \phi^2 \frac{u}{\beta + u} \tag{7}$$

with ϕ the Thiele modulus and subjected to the following :

$$\text{at} \quad \xi = 1 \quad -\frac{\partial u}{\partial \xi} = N_{Sh}(u - u_L) \tag{8a}$$

$$\xi = 0 \quad \frac{\partial u}{\partial \xi} = 0 \tag{8b}$$

When $\qquad\qquad \tau = 0 \quad u = 1 \quad 0 \leq \xi \leq 1 \tag{9}$

Where $\qquad\qquad \phi^2 = \frac{R^2 (k_O)_{max}\rho}{D_{eff}\,Co_{\varepsilon\phi\phi}} \qquad N_{Sh} = \frac{k_p R}{D_{eff}} \qquad \beta = \frac{K_m}{Co} \tag{10}$

with N_{Sh} the Sherwood number and u_L the dimensionless O_2 concentration when the external mass transfer resistance was not neglected.

From the mass balance in the pellet we obtain:

$$\frac{\partial u}{\partial \tau} = \frac{1}{\xi^2}\frac{\partial}{\partial \xi}\left(\xi^2 \frac{\partial u}{\partial \xi}\right) - \Re \tag{11}$$

with the reaction rate ($\Re$) defined by:

$$\Re = \phi^2 \frac{u}{\beta + u} \tag{12}$$

Whitaker (Whitaker, 1984; 1991) defines the volume-averaging function ($\overline{\Psi}$) as:

$$\overline{\Psi} = \frac{4\pi}{\frac{4}{3}\pi r_p^3}\int_0^{r_p}\Psi\, r^2 dr = 3\int_0^1 \Psi\, \xi^2 d\xi \tag{13}$$

with r_p the radius of one pellet (m) and Ψ. The mean O_2 concentration ($\overline{u}$) in the pellet was:

$$\overline{u} = 3\int_0^1 u\, \xi^2 d\xi \tag{14}$$

Substituting eq 14 in eq 11 gives:

$$\frac{\partial \overline{u}}{\partial \tau} = 3\int_{\xi=0}^{\xi=1}\frac{\partial}{\partial \xi}\left(\xi^2 \frac{\partial u}{\partial \xi}\right) - \overline{\Re}$$

$$\frac{\partial \overline{u}}{\partial \tau} = 3\xi^2 \frac{\partial u}{\partial \xi}\Big|_{\xi=0}^{\xi=1} - \overline{\Re} = 3\frac{\partial u}{\partial \xi}\Big|_{\xi=1} - \overline{\Re} = \frac{\partial \overline{u}}{\partial \tau} \tag{15}$$

and then the mean reaction rate ($\overline{\Re}$) is defined by :

$$\overline{\mathfrak{R}} = 3\int_0^1 \mathfrak{R}\,\xi^2\,\mathrm{d}\xi \qquad (16)$$

The effectiveness factor for O_2 consumption rate per unit of mycelial pellet (η) is defined as:

$$\eta = \frac{4\pi\int_0^1 \mathfrak{R}\xi^2\mathrm{d}\xi}{\frac{4}{3}\pi\mathfrak{R}\big|_{u_L}} = \frac{4\pi\int_0^{r_p} \mathfrak{R}R^2\mathrm{d}r}{\frac{4}{3}\pi R^3\mathfrak{R}\big|_{uL}} \qquad (17)$$

And
$$\eta = \frac{1}{\phi^2}\left(\frac{\beta+u_L}{u_L}\right)\overline{\mathfrak{R}} \qquad (18)$$

Using eq 15 and eq 18 gives:

$$\eta = \frac{1}{\phi^2}\left(\frac{\beta+u_L}{u_L}\right)\left(3\frac{\partial u}{\partial \xi}\Big|_{\xi=1} - \frac{\partial \overline{u}}{\partial \tau}\right) \qquad (19)$$

By solving eq 7 to 15, $\partial u/\partial \xi$ can be determined and used to calculate the effectiveness factor with eq 19. Eq 7 was discretized in radial direction with 13 orthogonal collocation points, using Legendre polynomials (Finlayson, 1980). The set of ordinary differential equations generated was solved with the Runge-Kutta-Fehlberg method with an adaptive control of each step.

Micro-organism. *Gibberella fujikuroi* (Sawada) strain CDBB H-984 conserved in potato glucose slants at 4ºC and sub-cultured every two months was used in the experiment (Culture collection of the Department of Biotechnology and Bioengineering, CINVESTAV-IPN, Mexico).

Culture medium. The culture medium contained 100 g of glucose l[-1], 3 g of NH_4Cl l[-1], 5 g of KH_2PO_4 l^{-1}, 1.5 g of $MgSO_4$ l[-1], 2 g of rice flour l[-1].

Culture conditions and equipment. The fungus was cultured on potato dextrose agar (PDA) slants at 29ºC for seven days. A 1000 ml Erlenmeyer flask containing 500 ml of medium was inoculated with spores and mycelium taken from the slants and incubated on a rotary shaker at 180 rpm and 29ºC for 36-38 h. A 30 dm³ turbine-agitated fermenter (Chemap A.G., Zurich) containing 20 dm³ of sterilized culture medium (pH 5) was inoculated with 5 % v/v of this culture. The aeration rate was 1 volume air volume[-1] of medium min^{-1} (vvm), the temperature and agitation-speed were automatically controlled at 29ºC and 700 rpm, respectively. pH and dissolved O_2, measured with three polarographic electrodes (Ingold, USA) installed at different depths in the culture medium, were monitored each h for 7 days. Every two h, 60 ml of medium was sampled and analysed for biomass, density (ρ) and diameter of the wet and dry pellet, reductive sugars, NH_4^+-N and gibberellic acid concentrations.

Pellets characterisation. The pellets in the sub-sample of the medium were filtered, washed twice with distilled H_2O and dried to constant weight at 90ºC in a vacuum-oven. The fermented broth was centrifuged in conical graduate tubes at 3000 rpm for 20 min and density, volume and weight of the wet pellets were determined while their diameter was measured with a microscope (Leica, MSD) on a calibrated micrometer grid. The pellets were vacuum dried at 90ºC for 16 h and their dry weight measured.

Volumetric mass-transfer coefficient (k_La). The gas flow rate was measured with a Brooks Mass controller 5851E while O_2 and CO_2 were monitored at the in and outlet with a paramagnetic O_2 analyser (Sybron 540A) and infrared CO_2 analyser (Sybron, Anatek PSA 402). The volumetric mass transfer coefficient obtained at maximum pellet concentration (k_La) (h^{-1}) was derived from the O_2 mass balance in the bioreactor (Sano et al. 1974).

O_2 uptake rate. Different concentrations of dissolved O_2 in the bioreactor were obtained by changing the compositions of the inlet air while keeping agitation speed and volumetric gas flow rate constant. The rate of O_2 uptake was determined by measuring the O_2 concentrations at the *in* and *outlet* and, as such, kinetics of O_2 were obtained without disturbing the system, i.e. power supply and gas hold-up (Wang and Fewkes, 1977).

Mixing time. The model assumed perfect mixing and two methods were used to verify this. First, the bioreactor with agitation speed of 700 rpm, a temperature of 29°C and an airflow of 1 vvm was filled with 0.1 M NaOH and phenolphthalein as a tracer. Samples were taken every 10 to 15 s at four different depths in the bioreactor (A, B, C, D), and analysed for absorbance at 550 nm (Figure 1). Second, a culture of *G. fujikuroi* in its maximum growth phase to which dextran blue was added as a tracer, was sampled every 10-15 sec at four different depths in the bioreactor and analysed for absorbance at 617.1 nm. Dextran blue was used as it is not affected by pH or by oxide-reduction processes, which take place during fermentation.

The distribution ages were determined by fitting the normalized equation (Levenspiel, 1999):

$$\int_0^\infty A dt = \int_0^\infty \frac{A}{Q} = dt \qquad (20)$$

To the dynamics of the tracer with $Q = \int_0^\infty A dt$ the area under the curve of absorbance. A is absorbance of the tracer and t is time. The mixing grade was determined by:

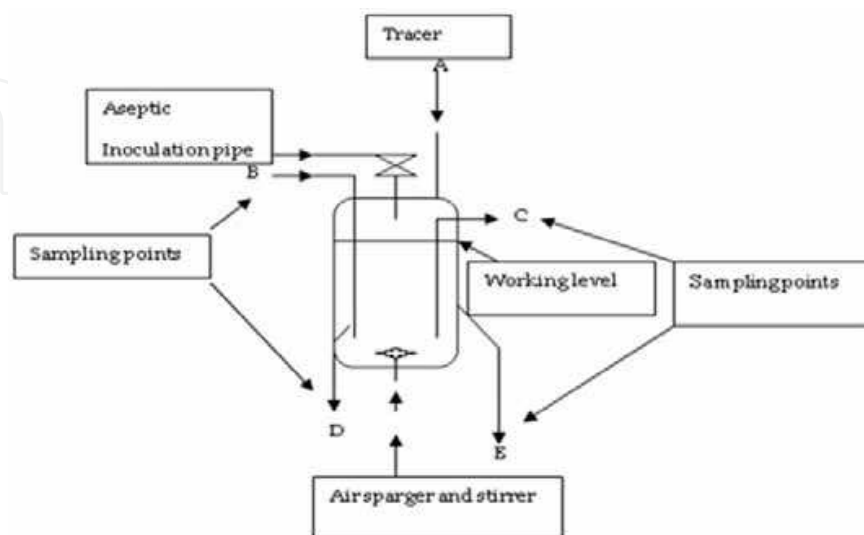$$m = \left(\frac{A - A_\infty}{A_\infty - A_0} \right) 100 \qquad (21)$$

Fig. 1. Diagram of the bioreactor

4.3 Parameter estimation

$k_L a$ determinations. The O_2 transfer rate (OTR) was derived from:

$$OTR = \frac{7.32 \times 10^5}{V_L} \left[\frac{Q_i \, P_i \, y_i}{T_i} - \frac{Q_o \, P_o \, y_o}{T_o} \right] \tag{22}$$

where 7.32×10^5 is a conversion factor (60 min h^{-1}) [mole (22.4 dm^3)$^{-1}$(standard conditions of Temperature and Pressure)] (273° K atm^{-1}), Q_i and Q_o is the volumetric air flow rate at the air in and outlet (dm^3 min^{-1}), P_i and P_o is the total pressure at the bioreactor air in and outlet (atm absolute), T_i and T_o is the temperature of the gases at the in and outlet (^{o}K), V_L is the volume of the broth contained in the vessel in dm^3, and y_i and y_o is the mole fraction of O_2 at the in and outlet (Wang et al. 1979).

The experimental values of $k_L a$ obtained from the *G. fujikuroi* culture were used to determine the volume fraction (θ_p) of the pellet using the empirical equation (Van Suijdam, 1982):

$$\frac{k_L a}{(k_L a)_0} = 0.5 \left[1 - \tanh \left(15\theta_p - 7.5 \right) \right] \tag{23}$$

with $(k_L a)_0$ the initial volumetric mass transfer coefficient (h^{-1}).

The liquid to pellet mass-transfer coefficient ($k_p a_p$) was calculated using the Sano, Yamaguchi and Adachi correlation (Sano et al. 1974). This correlation is based on Kolmoghorov's theory of local isotropic turbulence and is independent of the geometry of the equipment or the method energy input used. The Sherwood number N_{Sh} is:

$$N_{Sh} = 2.0 + 0.4 \left(N_{Re} \right)^{1/4} \left(N_{Sc} \right)^{1/3} \tag{24}$$

where N_{Re} is the Reynolds number and N_{Sc} the Schmidt number. N_{Sh} is given by:

$$N_{Sh} = \frac{k_p d_p}{D_{eff}} \tag{25}$$

with k_p is defined by eq (4a) and d_p is the diameter of the pellet (m). N_{Re} is defined as:

$$N_{Re} = \frac{\bar{\in} \, d_p^4}{\nu^3} \tag{26}$$

where $\bar{\in}$ is the mean of local energy dissipation per unit mass of suspension (W kg^{-1}) and ν is the kinematics viscosity of the suspending medium (9.18×10^{-6} m^2 s^{-1}). N_{Sc} is equal to νD_L^{-1} and approximately 3991 with D_L the molecular diffusion coefficient of dissolved O_2 in H_2O (m^2 h^{-1}).

$\bar{\in}$ in the impeller jet stream can be given as a function of the distance from the impeller shaft (r_{is}), the stirrer speed (N), and the stirrer diameter (D_R) (Van Suijdam and 1981, Metz):

$$\bar{\in} = \frac{0.86 N^3 D_R^6}{r_{is}^4} \tag{27}$$

$\bar{\epsilon}$ obtained was 140 W kg^{-1}; acceptable for inter-medium viscosity in the region of the impeller as the mycelial pellet suspensions showed Newtonian characteristics. The specific surface area of the these pellets (a_p) was estimated using

$$a_p = \frac{6\theta_p}{d_p} \tag{28}$$

The value for the liquid-solid mass transfer coefficient was estimated using eqs 25 to 30 with

$$\frac{dC_S}{dt} = k_P\, a_P \left(C_L - C_S \right) - \bar{k}_o \tag{29}$$

with $\bar{k}_o$ the mean O_2 consumption rate per unit of mycelial pellet (kg-moles of O_2 kg^{-1} of dry cell h^{-1}). Experimental radii, pellet density, maximal O_2 uptake rate and the effective diffusivity coefficient (D_{eff}) were used to calculate the Thiele modulus (eq 10).

O_2 uptake. The O_2 uptake rate was derived from the measured inlet gas flow rate ($\dot{V}_G^\alpha$), volume of the broth contained in the vessel (V_L), and gas compositions at the in and outlet using the gas balance taking into account the differences in inner and outlet gas flow rates:

$$k_o = \frac{\dot{V}_G^\alpha}{V_L} \left[Y_{O_2}^\alpha - Y_{O_2}^\omega \left(\frac{1 - Y_{O_2}^\alpha - Y_{CO_2}^\alpha}{1 - Y_{O_2}^\omega - Y_{CO_2}^\omega} \right) \right] \tag{30}$$

where Y_{O_2} and Y_{CO_2} are the volume fractions of O_2 and carbon dioxide in gas (α = inlet, ω = outlet).

Effective diffusivity estimation. Miura (Miura 1976) assumed that the effective diffusion coefficient is proportional to the void fraction within the pellet

$D_{eff} = D_L\, \epsilon$ (31)

with D_L being 9×10^{-6} m^2 h^{-1} at 29°C (Perry, 1997). Although eq 31 implies only the rectilinear paths inside the particles, similar results have been obtained with other empirical equations that consider tortuosity (Riley et al.. 1995; Riley et al. 1996) or intra-particle convection (Sharonet al. 1999).

Void fraction (ϵ) was defined as:

$$\epsilon = 1 - \frac{\rho_v}{\rho_c} \tag{31}$$

where ρ_c is the density of the dry pellet (kg m^{-3}) and ρ_v is the density of the wet pellet (kg m^{-3}). Both were experimentally determined.

The intrapellet Peclet number (Pe_{in}):

$$Pe_{in} \cong \left(\frac{\chi}{\epsilon} \right) Pe_{out} \tag{32}$$

was calculated to estimate the contribution of intrapellet convection (Parulekar and Lim,1985). The extra-Peclet number Pe_{out} is defined by:

$$Pe_{out} \cong \left(\frac{N_{Sh}}{0.6245} \right)^3 \qquad (33)$$

where the dimensionless number χ is defined as:

$$\chi = \frac{\kappa}{d_p^2} \qquad (34)$$

where κ is the hydraulic permeability of the pellet (m²) and estimated through Johnson's equation (Johnson and Kamm, 1987):

$$\frac{\kappa}{r_p^2} = 0.31 (\theta_p)^{-1.17} \qquad (35)$$

Numerical method. To fit the experimental oxygen uptake values with the non-linear ξ with parameters ϕ (involving $(k_o)_{max}$) and β (involving K_m), a least square algorithm coupled with the discretization of eq 7 via orthogonal collocation using Legendre polynomials and Runge-Kutta-Fehlberg methods was used (Jiménez-Islas et al. 1999). The set of non-linear equations derived in the minimization process, are solved with the Newton-Raphson method with LU factorisation. The optimization sequence is shown in Figure 2.
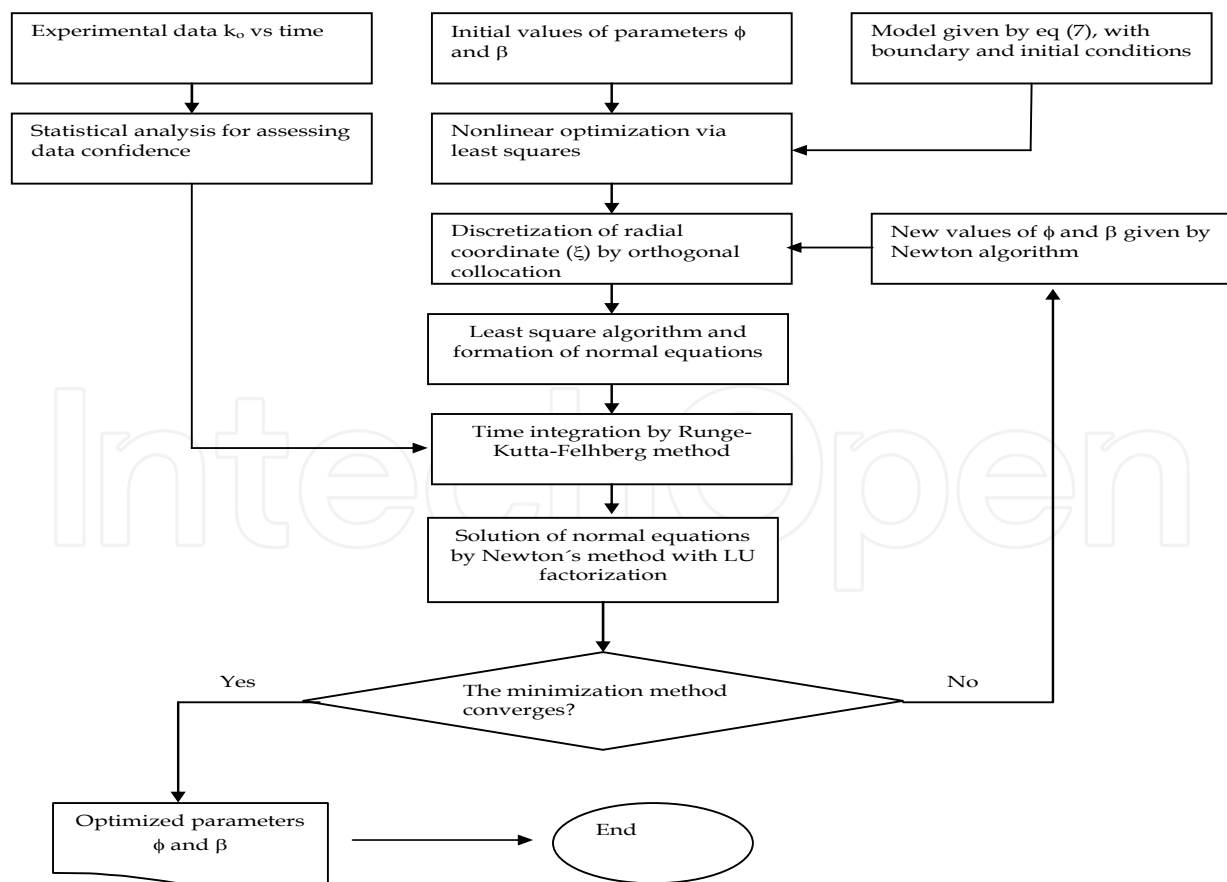

Fig. 2. Flow diagram for the optimization of the parameters ϕ and β (eq. 7).

4.4 Results and discussion

The bioreactor was well mixed (Figure 3). *G. fujikuroi* grew in dispersed mycelia (10%) or in the form of pellets (90%) within 38 h of culturing. The mean size of the pellets increased from 39 to 60 h and remained constant thereafter (Table I). The density of the pellets increased and gave a maximum after 82 h whereupon it decreased. O_2 uptake rates were simulated using eq 7 with a program specifically written for this purpose and the parameters were varied to fit the experimental data (Figure 4). These results included the resistance effects in the Michaelis-Menten equation (eq 3) not optimised before in this way. The estimated values for $(k_o)_{max}$ were $1.80 \times 10^{-4} \pm 3.05 \times 10^{-6}$ kg mole kg^{-1} dry cell h^{-1} and for K_m $2.49 \times 10^{-5} \pm 2.28 \times 10^{-6}$ kg-moles m^{-3} (Table II). These values are similar to those reported for *Aspergillus niger* (Miura et al.1975) and *Aspergillus orizæ* (Kim et al. 1983) but lower than
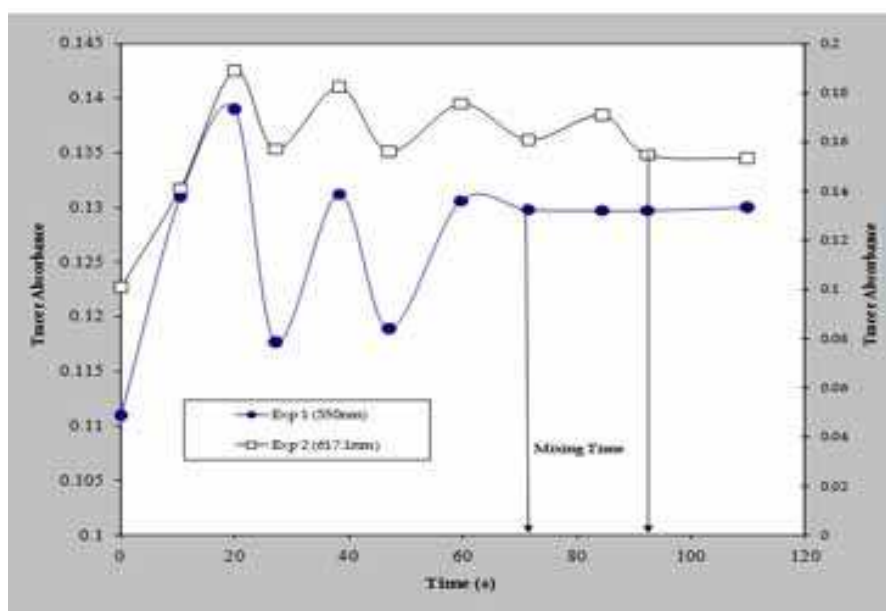

Fig. 3. Tracer absorbance of phenolphthalein measured at 550 nm (●) and dextran blue measured at 617.1 nm (□) used to verify the mixing behaviour in the bioreactor.

Fermentation time (h)	Size of the pellet ($\times 10^3$ m)	Pellet density (kg m^{-3})
39	1.50 (0.30)†	16.0 (0.90)
45	1.67 (0.40)	17.5 (0.75)
60	1.90 (0.32)	18.0 (0.50)
66	1.91 (0.28)	18.8 (0.23)
82	2.05 (0.51)	20.7 (0.45)
95	1.92 (0.40)	20.3 (0.30)
108	1.92 (0.30)	19.5 (0.45)
132	1.92 (0.29)	18.4 (0.23)
† values between parenthesis are standard deviations of five replicates		

Table I Size and density of *Gibberella fujikuroi* pellets during fermentation.

those obtained for *Penicillium chrysogenum* (Aiba, S.; Kobayashi,1975; Kobayashi et al. 1973). Differences between simulated and experimental data were less than 6 % and differences can be due to:

1. O_2 transfer rate in the mycelial pellet increases with agitation (Miura and Miyamoto 1977),
2. mycelial density is not uniform (Miura, 1976),
3. respiratory activity is not uniform in radial direction within the pellet (Wittler et al. 1986),
4. and internal convection (Sharon 1999).

The importance of each of these factors has not been assessed separately but they are indistinguishable in a model using D_{eff} and a homogeneous pellet. A summary of experimental and estimated parameters of O_2 diffusion in a bioreactor with *G. fujikuroi* (eq 7 to 34) is given in Table II. D_{eff} was derived from eqs 30 and 31 and is comparable to values reported in literature for other fungi. θ_p values below 30 % did not affect k_La values but they decreased when θ_p values were between 40 % and 60 % (Figure 5). The calculated θ_p value for pellets of *G. fujikuroi* was 39.8 % and allowed calculation of κ (eq 35) and Pe_{in} (eq 32). Pe_{in} for *G. fujikuroi* was 1.38 and κ was 8.22×10^{-7} m^2 (Table II). Stephanopoulos and Tsiveriotis (Sharon et al 1999) stated that the O_2 flow through the pellet does not affect the external mass transfer when Pe_{in} was close to 1 as found in this study. A constant D_{eff} can thus be assumed in our model. O_2 concentration derived from numerical solutions of eq 7 indicated that $\phi = 1$ gave an overall reaction rate of O_2 lower than the diffusion rate.

Parameter	value	Dimension	Remarks
d_p	2.090×10^{-3}	m	Experimental data
D_{eff}	4.15×10^{-6}	m^2 h^{-1}	estimated from eq 31
$\bar{\epsilon}$	139.96	W kg^{-1}	estimated from eq 27
K_m	2.49×10^{-5} (700 rpm)	kg mol O_2 m^{-3}	fitted from experimental data of Figure 4
$(k_o)_{max}$	1.80×10^{-4} (700 rpm)	kg mol O_2 h^{-1} kg^{-1} dry pellet	fitted from experimental data of Figure 4
k_La	91.93	h^{-1}	Experimental data
$(k_La)_o$	188.92	h^{-1}	Experimental data
N_{Re}	2.36×10^6	dimensionless	estimated from eq 26
κ	8.22×10^{-7}	m^2	estimated from eq 36
Pe_{out}	5.856	dimensionless	estimated from eq 34
Pe_{in}	1.38	dimensionless	estimated from eq 33
R	0.95×10^{-3}	m	Experimental data
N_{Sh}	250.6	dimensionless	estimated from eq 25
ϕ	1.12 to 2.4	dimensionless	estimated from eq 10
θ_p	0.398	dimensionless	estimated from Figure 5
ν	9.18×10^{-6}	m^2 s^{-1}	Experimental data
ρ	18.65	kg m^{-3}	Experimental data

Table II Summary of experimental and estimated parameters used for the solution of eqs 7 to 26.

The O_2 concentration did not change substantially in the pellet when $\phi > 5$ and the O_2 uptake was limited by diffusion and by mycelial activity. O_2 is then mostly consumed in the external core of the pellet.
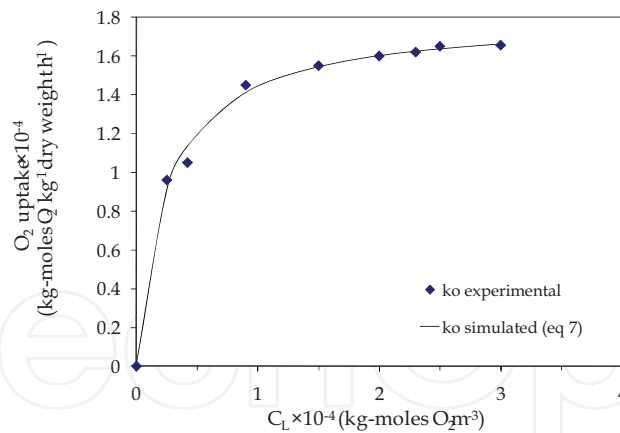
Fig. 4. Measured ($\blacklozenge$) and simulated (—) O_2 uptake (kg-moles kg^{-1} dry weight h^{-1}) by *Gibberella fujikuroi* in function of the O_2 dissolved in bulk liquid (kg-moles m^{-3}).
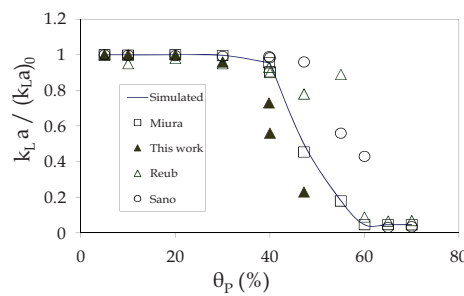

Fig. 5. Simulation of relationship between the dimensionless gas-liquid mass-transfer coefficient k_La $(k_La)_o{}^{-1}$ and the volume fraction of *Gibberella fujikuroi* pellets.

Experimental values for ϕ in fermentation with *G. fujikuroi* varied between 1.125 to 2.4 (Figure 6). The transport within the pellet depends on both diffusion and kinetics of the O_2 reaction. The mycelial activity in the inner zone of the pellet was reduced by O_2 limitation. Our model predicted that for $\phi<1.875$, η was close to 1 (Figure 7), consistent with other model predictions (Miura, 1976). Under these conditions, the respiratory activity is not limited by O_2 transport. For $\phi>1.875$, η is inversely proportional to ϕ. The estimated ϕ for *G. fujikuroi* indicated a small limitation of O_2 diffusion into the pellet. The large agitation rates and the small size of the pellet formed could explain this.
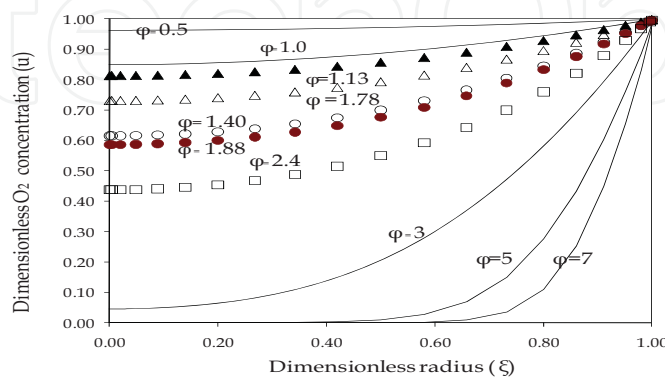

Fig. 6. O_2 concentration (u) in the pellet in function of the dimensionless radius (ξ) and the Thiele modulus (ϕ) with theoretical values of 0.5, 1.0, 3, 5 and 7 and other values calculated from experimental data 1.13 ($\blacktriangle$), 1.40 (Δ), 1.78 (o), 1.88 ($\bullet$), and 2.4 ($\square$).
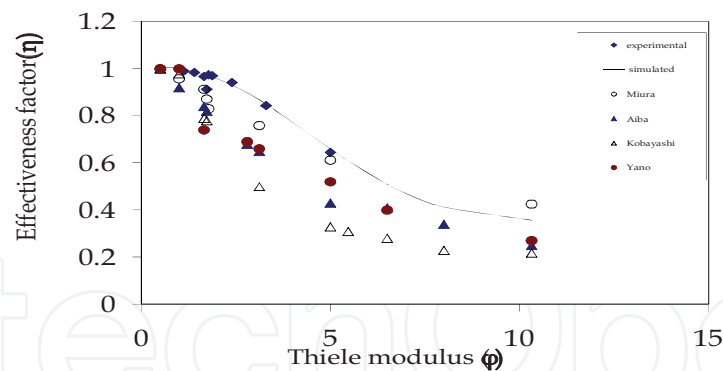
Fig. 7. Effect of Thiele Modulus (ϕ) on the effectiveness factor for mycelial pellets (η) as measured (♦) and simulated (—) in this experiment for *Gibberella fujikuroi* and as reported by Aiba et al. (*30*) (▲), Kobayashi et al. (*31*) (Δ), Miura et al. (*28*) (o) and Yano (*38*) (●).

Data from different authors were recalculated and expressed for ϕ in function of η (Figure 7). The effectiveness model was used to simulate those data and only η obtained with the data reported by Miura (Miura 1976) were comparable with those η values found in this experiment. A possible explanation is that Miura (Miura 1976) used a Michaelis-Menten type kinetic to calculate K_m and $(k_o)_{max}$ while the other authors used a zero and first-order kinetic resulting in values that were unrealistically large. η was not limited by transport for $\tau < 0.2$ (45.7 h) (Figure 8). After that, limitation of O_2 diffusion into the pellet started and a minimum for η was found for τ 0.8 (183.1 h). η remained constant thereafter (Wittler 1986).
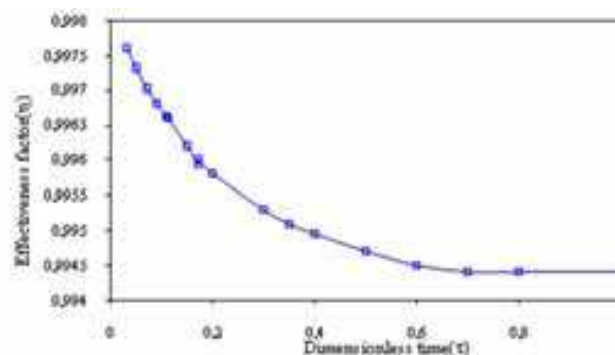

Fig. 8. Typical effectiveness factor through the dimensionless time for a representative experiment (pellet size ≥2 mm, air flow rate 1 vvm, 700 rpm, 29 °C, Thiele modulus 2.8).

4.5 Conclusions

Limitations in models simulating O_2 transfer into mycelial pellets with different strains of fungi have been reported, e.g. Sunil and Subhash, 1996; Miura, 1976; Aiba and Kobayashi, 197; Metz and Kossen, 1977; Chiam and Harris, 1981; Reuss et al. 1982; Nienow 1990. Explanations for these shortcomings can be related to unrealistically large values for D_{eff}, K_m and $(k_o)_{max}$ Experimental data of O_2 diffusion into pellets of *G. fujikuroi* were simulated satisfactorily. The O_2 reaction rate in pellets of 1.7-2.0 mm was only marginally inhibited by diffusion constraints under the conditions tested. Pe_{in} was small enough to justify a constant effective diffusivity and an isotropic pellet system with constant thermodynamic characteristics. O_2 transfer into the mycelial pellet can become the limiting factor in submerged fermentation of fungi when pellets larger than 2 mm are formed in the bioreactor. Eqs 7 and 19 allows to identify conditions critical for fermentations and to derive values for process parameters.

4.6 Nomenclature

a_P =   specific surface area of pellets (m^2)

C =   concentration of dissolved O_2 (kg-moles O_2 m^{-3})

C_O =   initial concentration of dissolved O_2 (kg-moles O_2 m^{-3})

C_L =   concentration of dissolved O_2 in bulk of liquid (kg-moles O_2 m^{-3})

C_S =   concentration of dissolved O_2 at liquid-pellet interface (kg-moles O_2 m^{-3})

d_P =   diameter of the pellet (m)

D_L =   molecular diffusion coefficient of dissolved O_2 in H_2O (m^2 h^{-1})

D_{eff} =   effective diffusivity coefficient of dissolved O_2 in mycelial pellet (m^2 h^{-1})

D_R =   stirrer diameter (m)

k_O =   specific O_2 uptake rate per unit dry mycelial weight (kg-moles of O_2 kg^{-1} of dry cell h^{-1})

$\bar{k_O}$ =   mean O_2 consumption rate per unit of mycelial pellet (kg-moles of O_2 kg^{-1} of dry cell h^{-1})

$(k_O)_{max}$ =   maximum specific O_2 consumption rate per unit dry mycelial weight (kg-moles of O_2 kg^{-1} of dry cell h^{-1})

k_P =   mass-transfer coefficient for the liquid film around cells or pellets defined by eq 4a (m h^{-1})

$k_P a_P$ =   liquid to pellet mass-transfer coefficient (m^2 h^{-1})

$k_L a$ =   volumetric mass transfer coefficient obtained at maximum pellet concentration (h^{-1})

$(k_L a)_0$ =   initial volumetric mass transfer coefficient (h^{-1})

K_m =   apparent Michaelis constant for mycelia (kg-moles m^{-3})

N =   stirrer speed (rpm)

N_{Re} =   Reynolds number

N_{Sc} =   Schmidt number

N_{sh} =   Sherwood number

Pe_{in} =   intraparticle Peclet number $\left(\dfrac{\chi}{(\varepsilon)}\right) Pe_{out}$

Pe_{out} =   extra-Peclet number $\left(\dfrac{N_{Sh}}{0.6245}\right)^3$

$P_i P_o$ =   the total pressure at the bioreactor air in and outlet (atm absolute),

$Q_i Q_o$ =   the volumetric air flow rate at the air in and outlet (dm^3 min^{-1})

r =   radial distance from centre of mycelial pellet (m)

R =   radius of mycelial pellet (m)

r_{is} =   radius from the impeller shaft (m)

r_p =   radius of one pellet (m)

t =   time (h)

$T_i T_o$ =   the temperature of the gases at the in and outlet (^oK)

u =   dimensionless concentration of O_2 defined in eq 6

$\bar{u}$ =   dimensionless mean concentration of O_2 defined in eq 14

u_L =   dimensionless O_2 concentration when the external mass transfer resistance was not neglected defined in eq 8a

$\dot{V}_G^\alpha$ =   gas flow rate (m^3 h^{-1})

V_L = volume of broth contained in the vessel (dm^3)

$y_i\ y_o$ is the mole fraction of O_2 at the in and outlet

$Y_{O_2}^{\alpha}$
$Y_{O_2}^{\omega}$ = are the volume fractions of O_2 in gas (α = inlet, ω = outlet)

$Y_{CO_2}^{\alpha}$
$Y_{CO_2}^{\omega}$ = are the volume fractions of CO_2 in gas (α = inlet, ω = outlet)

Greek

β = constant defined in eq 10 (dimensionless)
ε = void fraction (dimensionless)
$\overline{\in}$ = mean local energy dissipation per unit mass (W kg^{-1})
θ_p = volume fraction of pellets (dimensionless)
ξ = ratio of radial distance to radius of the pellet (dimensionless)
κ = effective hydraulic permeability of the pellet (m^2)
η = Effectiveness factor for O_2 consumption rate per unit mycelial pellet (dimensionless)
ρ_c = density of the dried pellet (kg m^{-3})
ρ_v = density of wet pellet (kg m^{-3})
ρ = pellet suspension density (kg m^{-3})
τ = dimensionless time defined in eq 6
ϕ = Thiele modulus (dimensionless)
ν = kinematics viscosity of the suspending medium ($m^2\ s^{-1}$)
χ = dimensionless parameter defined in eq 35
$\overline{\Re}$ = mean reaction rate defined in eq 16
$\Re$ = reaction rate defined by eq 12
Ψ = volume function
$\overline{\Psi}$ = volume averaging function defined in eq 13

umerical values for process parameters.

5. Reference

5.1 References cited in Case I

Abashar, M. E., Narsingh, U., Rouillard, A. E. and Judd, R. (1998). Hydrodynamic flow regimes, gas holdup, and liquid circulation in *airlift* reactors. *Ind. Eng. Chem. Res.* 37: 1251-1259.

Akita, K. and Yoshida, F. (1973). Gas holdup and volumetric mass transfer coefficient in bubble columns. Effects of liquid properties. *Ind. Eng. Chem. Process Des. Develop.* 12: 76-80.

Al-Masry, W. A.. and Dukkan, A. R. (1998). Hydrodynamics and mass transfer studies in a pilot-plant *airlift* reactor: non-Newtonian systems. *Ind. Eng. Chem. Res.* 37: 41-48.

Barboza, M., Zaiat, M. and Hokka, C.O. (2000). General relationship for volumetric oxygen transfer coefficient (k_La) prediction in tower bioreactors utilizing immobilized cells. *Bioprocess Eng.* 22: 181-184.

Barrow, A., Jefferys, E. G. and Nixon, I. S. (1960). Process for the production of gibberellic acid. ICI Patent. GB 838,032.

Brito-De la Fuente, E., Nava, J. A., López, L. M., Medina, L., Ascanio, G. and Tanguy, P. A. (1998). Process viscometry of complex fluids and suspensions with helical ribbon agitators. *Can. J Chem. Eng.* 76: 689-695.

Brückner, B. and Blechschmidt, D. (1991). The Gibberellin Fermentation. *Crit. Rev. Biotech.* 11, 163-192.

Chavez Parga, M. C. (2005). "Producción de ácido giberélico en un biorreactor *airlift*". Ph. D. Thesis. Instituto Tecnológico de Celaya. Celaya, Gto., México.

Chisti, M. Y. (1989). *Airlift bioreactor*. London-New York: Elsevier Appl. Science.

Choi, K. H., Chisti, Y. and Moo-Young, M. (1996). Comparative evaluation of hydrodynamic and gas-liquid mass transfer characteristics in bubble column and airlift slurry reactors. *Biochem. Eng. J* 62:223-229.

Escamilla-Silva, E. M., Dendooven, L., Magaña, I. P., Parra-Saldivar, R. and De la Torre, M. (2000). Optimization of Gibberellic acid production by immobilized *Gibberella fujikuroi* mycelium in fluidized bioreactors. *J Biotechnol.* 76:147-155.

Freitas, C. and Teixeira, J. A. (1998). Hydrodynamic studies in an *airlift* reactor with an enlarged degassing zone. *Bioprocess Eng.*18: 267-279.

Gelmi, C., Pérez-Correa, R., González, M. and Agosin, E. (2000). Solid substrate cultivation of *Gibberella fujikuroi* on an inert support. *Process Biochem.* 35:1227-1233.

Gelmi, C., Pérez-Correa, R. and Agosin, E. (2002). Modelling *Gibberella fujikuroi* growth and GA$_3$ production in solid-state fermentation. *Process Biochem.* 37:1033-1040.

Godbole, S. P., Schumpe, A., Shah, T. and Carr, N. L. (1984). Hydrodynamics and mass transfer in non-Newtonian solutions in a bubble column. *AIChE J* 30: 213-220.

Gouveia, E. R., Hokka, C. O. and Badino-Jr, A. C. (2003). The effects of geometry and operational conditions on gas holdup, liquid circulation and mass transfer in an airlift reactor. *Braz. J Chem. Eng.* 20:363-374.

Gravilescu, M. and Tudose, R. Z. (1998). Hydrodynamics of non-Newtonian liquids in external-loop *airlift* bioreactor. Part I. Study of the gas holdup. *Bioprocess. Eng.* 18:17-26.

Gravilescu, M. and Tudose, R. Z. (1999). Modelling mixing parameters in concentric-tube airlift bioreactors. Part I. Mixing time. *Bioprocess Eng.* 20:423-428.

Halard, B., Kawase, Y. and Moo-Young, M. (1989). Mass transfer in a pilot plant scale *airlift* column with non-Newtonian fluids. *Ind. Eng. Chem. Res.* 28: 243-245.

Heinrich, M. and Rehm, H. J. (1981). Growth of *Fusarium moniliforme* on n-alkanes: comparison of an immobilization method with conventional processes. *Eur. J Appl. Microbiol. Biotechnol.* 11:239.

Jones, A. and Pharis, R. P. (1987). Production of gibberellins and bikaverin by cells of *Gibberella fujikuroi* immobilized in carrageenan. *J Ferment. Technol.* 65:717-722.

Kawase, Y. (1989). Liquid circulation in external-loop airlift bioreactors. *Biotechnol. Bioeng.* 35:540-546.

Kumar, P. K. P. and Lonsane, B. K. (1987) Gibberellic acid by solid state fermentation: consistent and improved yields. *Biotechnol. Bioeng.* 30:267-271.

Kumar, P. K. P. and Lonsane, B. K. (1988) Immobilized growing cells of *Gibberella fujikuroi* P-3 for production of gibberellic acid and pigment in batch and semi-continuous cultures. *Appl. Microbiol. Biotechnol.* 28:537-542.

Metz, B., Kossen, N. W. F. and van Suijdam, J. C. (1979). The rheology of mould suspensions. *Adv. Biochem. Eng*. 11:103-156.

McManamey, W. J. and Wase, D. A. J. (1986). Relationship between the volumetric mass transfer coefficient and gas holdup in *airlift* fermentors. *Biotechnol. Bioeng*. 28:1446-1448.

Moo-Young, M., Halard, B., Allen, D. G., Burrell, R. and Kawase, Y. (1987). Oxygen transfer to mycelial fermentation broths in an airlift fermentor. *Biotechnol. Bioeng*. 30:746-753.

Nava Saucedo, J. E., Barbotin, J. N. and Thomas, D. (1989). Continuous production of gibberellic acid in a fixed-bed reactor by immobilized mycelia of *Gibberella fujikuroi* in calcium alginate beads. *Appl. Microbiol. Biotechnol*. 30:226-233.

Prokop, A., Janík, P., Sobotka, M. and Krumphanzi, V. (1983). Hydrodynamics, mass transfer, and yeast culture performance of a column bioreactor with ejector. *Biotechnol. Bioeng*. 25: 114-1160.

Quintero, R. R. (1981). *Ingeniería bioquímica, Teoría y aplicaciones*. Ed. Alambra. México.

Schügerl, K., Lücke, J. and Oels, U. (1977). Bubble column bioreactors. *Adv. Biochem. Eng*. 7:1-81.

Shah, Y. T., Kelkar, B. G., Godbole, S. P. and Deckwer, W. D. (1982). Design parameters estimations for bubble column reactors. *AIChE J* 28:353-379.

Shukla, R., Srivastava, A. K. and Chand, S. (2003). Bioprocess strategies and recovery processes in gibberellic acid fermentation. *Biotechnol. Bioprocess Eng*. 8:269-278.

Tobajas, M. and García-Calvo, E. (2000). Comparison of experimental methods for determination of the volumetric mass transfer coefficient in fermentation processes. *Heat and mass transfer* 36: 201-207.

Tudzynski, B. (1999). Biosynthesis of gibberellins in *Gibberella fujikuroi*: biomolecular aspects. *Appl. Microbiol. Biotechnol*. 52:298-310.

5.2 References cited in Case II

Beydilli M I, Pavlostasthis S G. (2005). Decolorization kinetics of the azo dye Reactive Red 2 under methanogenic conditions: effect of long-term culture acclimation. Biodegradation. 16: 135–146.

Van der Zee F P, Bisschops I A E, Lettinga G. (2003). Activated carbon as an electron acceptor and redox mediator during the anaerobic biotransformation of azo dyes. Environ Sci Technol. 37: 402-408.

Beyenal H, Lewandowski Z. (2002). Internal and external mass transfer in biofilms grown at various flow velocities. Biotechnol Prog. 18: 55-61.

Fan L S, Fujie K, Long T R, Tang W T. (1987). Characteristics of draft tube gas-liquid-solid fluidized-bed bioreactor with immobilized living cells for phenol degradation. Biotechnol Bioeng. 30: 498-504.

Fan L-S, Leyva-Ramos R, Wisecarver K D, Zehner B J. (1990). Diffusion of phenol through a biofilm grown on activated carbon particles in a draft-tube three-phase fluidized-bed biorreactor. Biotechnol Bioeng. 35: 279-286.

Herzberg M, Dosoretz C G, Tarre S, Green M. (2003). Patchy biofilm coverage can explain the potential advantage of BGAC reactors. Environ Sci Technol. 37: 4274-4280.

McCarty P L, Meyer T E. (2005) Numerical model for biological fluidized-bed reactor treatment of perchlorate-contaminated groundwater. Environ Sci Technol. 39: 850-858.

Di Iaconi C, Ramadori R, Lopez A, Pasión R. (2005). Hydraulic shear stress calculation in a sequencing batch biofilm reactor with granular biomass. Environ Sci Techno. l39: 889-894.

Iliuta I, Thyrion F C, Muntean O, Giot M. (1996). Residence time distribution of the liquid in gas-liquid cocurrent upflow fixed-bed reactors. Chem Eng Sci. 51(20): 4579-4593.

Smith L C, Elliot D J, James A. (1996). Mixing in upflow anaerobic filters and its influence on performance and scale-up. Water Res. 30(12): 3061-3073.

Levenspiel O. Chemical reaction engineering (Spanish translation). 3rd Ed. México: Limusa Wiley; 2004. p. 668.

Fogler H S. Elements of chemical reaction engineering, 3rd Ed. New Jersey, USA: Prentice Hall PTR; 1999. p. 967.

Escamilla-Silva E M, Gutierrez G F, Dendooven L, Jimenez-Islas H, Ochoa-Tapia J A. (2001). A Method to Evaluate the Isothermal Effectiveness Factor for Dynamic Oxygen into Mycelial Pellets in Submerged Cultures. Biotechnol Prog.17(1): 95-103.

Kulkarni R R, Wood J, Winterbottom J M, Stitt E H. (2005). Effect of fines and porous catalyst on hydrodynamics of trickle bed reactors. Ind Eng Chem Res; 44(25): 9497-9501.

Hines A L, Maddox R N. Mass transfer, fundamentals and applications (spanish translation). México: Prentice Hall Hispanoamericana; 1987. p. 600.

Lee J-W, Choi S-P, Thiruvenkatachari R, Shim W-G, Moon H. (2006). Evaluation of the performance of adsorption and coagulation processes for the maximum removal of reactive dyes. Dyes and Pigments. 69: 196-203.

Chen K-C, Wu J-Y, Yang W-B, Hwang S-C J. Evaluation of Effective Diffusion Coefficient and Intrinsic Kinetic Parameters on Azo Dye Biodegradation Using PVA-Immobilized Cell Beads. Biotechnol Bioeng 2003; 83(7): 821-832.

Iliuta I, Larachi F. (2005). Modeling simultaneous biological clogging and physical plugging in trickle-bed bioreactors for wastewater treatment. Chem Eng Sci. 60: 1477 – 1489.

Spigno G, Zilli M, Nicolella C. (2004). Mathematical modelling and simulation of phenol degradation in biofilters. Biochem Eng J. 19: 267–275.

Mammarella E J, Rubiolo A C. (2006). Predicting the packed-bed reactor performance with immobilized microbial lactase. Process Biochem. 41: 1627–1636.

Leitão A, Rodriguez A. (1996). Modeling of biodegradation/adsorption combined processes in fixed-bed biofilm reactors: effects of the intraparticle convective flow. Chem Eng Sci. 51(20): 4595 4604.

Leitão A, Rodriguez A. Dynamic behavior of a fixed-bed biofilm reactor: analysis of the role of the intraparticle convective flow under biofilm growth. Biochem Eng J 1998; 2: l-9.

Lewandowski Z, Stoodley P, Altobelli S, Fukushima E. (1994). Hydrodynamics and kinetics in Biofilm systems - Recent advances and new problems. Wat Sci Tech. 29(10-11): 223-229.

5.3 References cited in Case III

Takamatsu, T.; Shioya, S.; Furuya, T. (1981). Mathematical Model for Gluconic Acid Fermentation by *Aspergillus niger*. *J Chem. Tech. Biotechnol. 31*, 697-704.

Qian, X.M.; du Preez, J.C.; Kilian, S. G. (1994). Factors Affecting Gibberellic Acid Production by *Fusarium moniliforme* in Solid-State Cultivation on Starch. *World J Microbiol. Biotechnol*. *10*, 93-99.

Lu, Z.X.; Xie, Z.C.; Kumakura, M. (1995). Production of Gibberellic Acid in *Gibberella fujikuroi* Adhered onto Polymeric Fibrous Carriers. *Process Biochem. 30*, 661-665.

Hollmann, D.; Switalski, J.; Geipel, S.; Onken, U. (1995). Extractive Fermentation of Gibberellic Acid by *Gibberella fujikuroi*. *J Ferment. And Bioeng*.*79*, 594-600.

el-Enshasy, H., Hellmuth, K., Rinas U. (1999). Fungal morphology in submerged cultures and its relation to glucose oxidase excretion by recombinant *Aspergillus niger*. Appl. Biochem. Biotechnol., *81*, 1-11.

Yamane, T.; Shimizu, S. (1984). Fed-batch techniques in microbial processes. In: Fiechter A. Ed.: *Adv. Biochem. Eng. /Biotechnol.*, *30*, 147-194.

Wang, N. S.; Stephanopoulos, G. (1984). Computer Applications for Fermentations Processes. *CRC Critical Reviews in Biotechnology*. *2*, 1-103.

Parulekar, S. J.; Lim, H.C. (1985). Modelling Optimization and Control of Semi-Batch Bioreactors. In: Fiechter A.(De.): *Adv. Biochem. Eng. /Biotechnol. 32*, 207-258.

Sharon, C., Nakazato, M., Ogawa H.I., Kato Y. (1999). Bioreactor operated production of lipase: castor oil hydrolysis using partially-purified lipase. Indian. J. Exp. Biol. *37*, 481-486.

Stephanopoulos, G.; Tsiveriotis, K. (1989). The Effect of Intraparticle Convection on Nutrient Transport in Porous Biological Pellets. *Chem. Eng. Sci. 44*, 2031-2039.

Reuss, M.; Fröhlich, S.; Kramer, B.; Messerschmidt, K.; Pommerening, G. (1986). Coupling of Microbial Kinetics and oxygen transfer for Analysis and Optimization of Gluconic Acid Production with *Aspergillus niger*. *1*,79-91.

Nielsen, J.; Villadsen, J. In *Bioreaction Engineering Principles*. Plenum Press: New York 1994.

Sunil, N.; Subhash, Ch. (1996). Mass Transfer and Biochemical Reaction in Immobilised Cell Packed Bed Reactors: Correlation of Experimental with Theory. *J Chem. Tech. Biotechnol. 66*, 286-292.

Cui, Y.Q., van der Lans, R.G., Luyben, K.C. (1998). Effects of dissolved oxygen tension and mechanical forces on fungal morphology in submerged fermentation. Biotechnol. Bioeng. 57, 409-410

Goosen, M.F. (1999). Physico-chemical and mass transfer considerations in micro-encapsulation. Ann. N. Y. Acad. Sci. *875*, 84-104.

Fan, D., Shang, L., Yu, J. (1996). Research on fermentation scale-up based on the OUR obtained from a shake flask. Chin. J. Biotechnol. *12*, 177-184.

Carbonell, R. G.; Whitaker S. Heat and mass transfer in porous media. In *Fundamentals of Transport in Porous Media*; Bear, J.; Corapcioglu, M. Y. Eds.; Martinus Nijhoff: Brussels, 1984; pp 121-198.

Ochoa, J.A.; Strove P.; Whitaker, S. (1986). Diffusion and Reaction in Cellular Media. *Chem. Eng. Sci. 41*, 2999-3013.

Whitaker, S. (1991). Improved Constraints for the Principle of Local Equilibrium. *I & E C Research. 29*, 983-997.

Aris, R. The Mathematical Theory of Diffusion and Reaction in Permeable Catalysts. Vol.1, The theory of the Steady State; Vol.2, Questions of Uniqueness, Stability and Transient Behaviour; Clarendon Press: Oxford, 1975.

Whitaker, S. Flow in Porous Media I: A Theoretical Derivation of Darcy's Law. *Transport in Porous Media.* 1986, *1*, 3-25.

Finlayson, B. A. *Nonlinear Analysis in Chemical Engineering.* McGraw-Hill Book Co.: USA, 1980.

Sano, Y.; Yamaguchi, N.; Adachi, T. (1974). Mass Transfer Coefficients for Suspended Particles in Agitated Vessels and Bubble Columns. *J Chem. Eng. Jpn. 7*, 255-261.

Wang, D. I. C.; Fewkes, R. C. Mass Transfer Studies in Fermentation Broths. *J Dev. Ind. Microbiol*. 1977, *18*, 39-44.

Levenspiel O. *Chemical Reaction Engineering.* Wiley International, Second Edition, 1972.

Wang, D. I. C.; Cooney, C. L.; Demain, A. L.; Dunnill., P.; Humphrey, A. E.; Lilly, M. D. Fermentation and Enzyme Technology. Wiley, N.Y. 1979.

Van Suijdam, J. C.; Hols, H.; Kosen, N. W. F. (1982). Unstructured Model for Growth of Mycelial Pellets in Submerged Cultures. Biotechnol. Bioeng. 24, 177-191.

Van Suijdam, J. C.; Metz, B. (1981). Influence of Engineering Variables upon the Morphology of Filamentous Molds. *Biotechnol. Bioeng. 23*, 111-148.

Miura, Y. (1976). Transfer of Oxygen and Scale-Up in Submerged Aerobic Fermentation. *Adv. Biochem. Eng. 4*, 1-40.

Perry, H. R.; Green, Don W.; Maloney, J.O. *Perry's Chemical Engineers Handbook;* Mc Graw-Hill: New York, 1997.

Riley, M. R.; Muzzio F. J.; Buettner H. M.; Reyes, S. C. (1995). A Diffusion in Heterogeneous Media: Applications to Immobilized Cell Systems. *AIChE J 41*, 691-700.

Riley, M. R.; Muzzio, F. J.; Buettner, H. M.; Reyes S. C. (1996). A Simple Correlation for Predicting Effective Diffusivities in Immobilized Cell Systems. *Biotechnol. Bioeng*. *49*, 223-227.

Johnson, M. R.; Kamm, C. R.; Ethier, T. P. (1987). Scaling Laws and the Effects of Concentration Polarization on the Permeability of Hyaluronic Acid. PhysicoChem. Hydrody. 9, 427.

Jiménez-Islas, H., López-Isunza, F., Ochoa-Tapia, J.A. (1999). Natural convection in a cylindrical porous cavity with internal heat source: a numerical study with Brinkman-extended Darcy model. *Int. J Heat Mass Transfer. 42*, 4185-4195.

Miura, Y.; Miyamoto, K.; Kanamori, T.; Ohira, N. (1975). Oxygen Transfer within Fungal Pellets. *J Chem. Eng. Jpn. 8*, 300-304.

Kim. J. H., Lebeault, J. M., Reuss, M. (1983). Comparative Study of Rheological Properties of Mycelial Broth in Filamentous and Pelleted Forms. Eur. J. App. Microbiol. Biotechnol. *18*, 11-23.

Aiba, S.; Kobayashi, K. (1971). Comments on Oxygen Transfer Within a Mold Pellet. *Biotechnol. Bioeng. 15*, 27-29.

Kobayashi, T.; Van Dedem, G.; Moo-Young, M. (1973) Oxygen Transfer Into Mycelial Pellets. *Biotechnol. Bioeng. 15*, 27-32.

Miura, Y.; Miyamoto, K. (1977). Oxygen Transfer within Fungal Pellets. *Biotechnol. Bioeng*. *19*, 1407-1409.

Wittler, R.; Baumgartl, H.; Lübbers, D.W.; Schürgerl, K.(1986). Investigations of Oxygen Transfer into *Penicillium chrysogenum* Pellets by Microprobe Measurement. *Biotechnol. Bioeng. 28*, 1024-1036.

Metz, B.; Kossen, N. W. F. (1977). The Growth of Molds in the Form of the Pellets A Literature Review. *Biotechnol. Bioeng. 19*, 781-799.

Chiam, H. F.; Harris I. J. (1981). Microelectrode Studies of Oxygen Transfer in Trickling Filter Slimes. *Biotechnol. Bioeng.* *23*, 781-792.

Reuss, M.; Bajpai, R. K.; Berke, W. (1982). Effective Oxygen-Consumption Rates in Fermentation Broths with Filamentous Organisms. *J Chem. Tech. Biotechnol.* *32*, 81-91.

Nienow, A. W. 1990. Agitation for Mycelial Fermentations. *Trends Biotechnol.* *8*, 224-233.

Yano, T., Kodama, T., Yamada, K. (1961). Fundamental Studies on the Aerobic Fermentation. *Agr. Biol. Chem.* 25(7), 580-584.

Huang, M.Y.; Bungay, H.R. (1973).Microprobe Measurements of Oxygen Concentration in Mycelial Pellets. *Biotechnol. Bioeng.* *15*, 1193-1201.

Ngian, K. F.; Lin S. H. (1976). Diffusion Coefficient of Oxygen in Microbial Aggregates. *Biotechnol. Bioeng.* *18*, 1623-1627.

Fan, L.S.; Leyva Ramos, R.; Wisecarver, K. D.; Zehener, B. J. (1990). Diffusion of Phenol through a Biofilm Grown on Activated Carbon Particles in a Draft-Tube Three-Phase Fluidized-Bed Bioreactor. *Biotechnol. Bioeng.* *39*, 279-286.

Ross, L. W.; Updegraff, D. M. (1971). Kinetics of Diffusion-Coupled Fermentation Processes: Conversion of Cellulose to Protein. *Biotechnol. Bioeng.* *13*, 99-111.
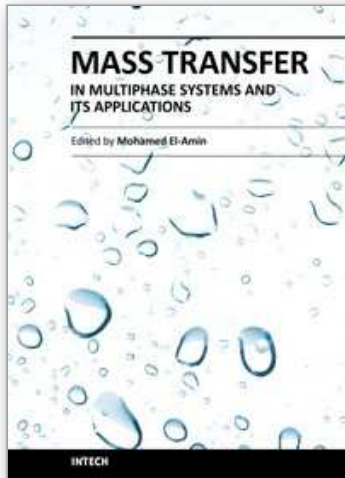
Mass Transfer in Multiphase Systems and its Applications

Edited by Prof. Mohamed El-Amin

ISBN 978-953-307-215-9

Hard cover, 780 pages

Publisher InTech

Published online 11, February, 2011

Published in print edition February, 2011

This book covers a number of developing topics in mass transfer processes in multiphase systems for a variety of applications. The book effectively blends theoretical, numerical, modeling and experimental aspects of mass transfer in multiphase systems that are usually encountered in many research areas such as chemical, reactor, environmental and petroleum engineering. From biological and chemical reactors to paper and wood industry and all the way to thin film, the 31 chapters of this book serve as an important reference for any researcher or engineer working in the field of mass transfer and related topics.

How to reference

In order to correctly reference this scholarly work, feel free to copy and paste the following:

Ma. del Carmen Chávez, Linda V. González, Mayra Ruiz, Ma. de la Luz X. Negrete, Oscar Martín Hernández and Eleazar M. Escamilla (2011). Mass Transfer in Bioreactors, Mass Transfer in Multiphase Systems and its Applications, Prof. Mohamed El-Amin (Ed.), ISBN: 978-953-307-215-9, InTech, Available from: http://www.intechopen.com/books/mass-transfer-in-multiphase-systems-and-its-applications/mass-transfer-in-bioreactors

INTECH
open science | open minds